Paul A. Bottomley, PhD

Human in Vivo NMR Spectroscopy in Diagnostic Medicine: Clinical Tool or Research Probe?[1]

In this critical review of human in vivo nuclear magnetic resonance (NMR) spectroscopy, the questions of which chemical species can be detected and with what sensitivity, their biochemical significance, and their potential clinical value are addressed. The current in vivo detectability limit is about 10^{-6} of that of tissue water protons, necessitating a 1-10 cm^3-volume of tissue and ~10-minute averaging time. This permits access to fats, membrane lipid metabolism, high-energy phosphate metabolism, glycogen, some neurotransmitters and metabolites in the citric acid cycle, and artificially introduced fluorocompounds. While hydrogen-31, phosphorus-31, carbon-13, sodium-23, and fluorine-19 in vivo results are discussed, the majority of patient studies use P-31 NMR spectroscopy. Here results from metabolic and ischemic disorders substantiate a case for spectroscopy as a diagnostic modality. The use of a broad range of spatial localization strategies is justifiable on the basis of the location and size of the pathologic condition and of NMR sensitivity. Abnormalities in spectra from many other disorders, most notably cancer, and improvements are often observed early in the course of successful therapy. Yet the potential impact of these results on clinical diagnosis and therapeutic monitoring is not always well understood, and many questions remain. Neurotransmitters and citric acid cycle metabolites exhibit high H-1 NMR sensitivities and represent major untapped potential for human clinical spectroscopy research. Studies evaluating spectroscopy in the context of existing modalities are needed. The unique ability of spectroscopy to provide noninvasive information about tissue chemistry in patients bodes well for its impact on clinical research and disease diagnosis.

Abbreviations

n-AcAsp	n-acetyl aspartate
ADP	adenosine diphosphate
AF	audio frequency
β-ATP	(beta) adenosine triphosphate
1-3D	one to three dimensional
2-4DFT	two to four dimensional Fourier transform
DRESS	depth-resolved surface coil spectroscopy
FDG	2-fluoro-2-deoxy-d-glucose
FID	free induction decay
GABA	γ-aminobutyrate
GPC	glycerophosphorylcholine
GPE	glycerophosphorylethanolamine
ISIS	image-selected in vivo spectroscopy
NAD	nicotinamide adenine dinucleotide
NADH	reduced NAD
NOE	nuclear Overhauser enhancement
PCh	phosphorylcholine
PCr	phosphocreatine
PD	phosphodiester
PEt	phosphorylethanolamine
PFTB	perfluorotributylamine
Pi	inorganic phosphate
PM	phosphomonoester
RF	radio frequency
RFZ	rotating frame zeugmatography
S/N	signal-to-noise ratio
TMR	topical magnetic resonance

Index terms: Magnetic resonance (MR), phosphorus studies • Magnetic resonance (MR), spectroscopy • State-of-Art reviews

Radiology 1989; 170:1-15

WHEREAS magnetic resonance (MR) imaging is an anatomic imaging modality in a long tradition of anatomic imaging techniques in radiology, nuclear magnetic resonance (NMR) spectroscopy is unique. It is the *only* technique in clinical medicine that provides noninvasive access to living chemistry in situ. This is the root of both the great excitement and intensity of effort devoted to clinical in vivo spectroscopy research (just about any clinical spectroscopic study one does is new!), as well as the perceived delay in identifying *real* clinical applications. Why is clinical spectroscopy so tardy in its delivery? In introducing this new technology in diagnostic medicine, MR spectroscopists face four major challenges: (*a*) proving technical feasibility in a clinical environment, (*b*) interpreting and understanding new chemical information from patients in the context of modern biochemistry, (*c*) quantifying differences between normal and disease states, and (*d*) applying spectroscopic information to efficacious disease diagnosis in the contexts of existing techniques and benefit to the patient. It is not that spectroscopy is more tardy but rather that its path to delivery is longer.

Here I critically review clinical research in human in vivo NMR spectroscopy, detailing findings from published human proton (H-1), phosphorus (P-31), carbon (C-13), sodium (Na-23), and fluorine (F-19) NMR studies and identifying questions, problems, and potentially fertile areas that are as yet untapped. Through examples, a strong case is made that spectroscopy has met all four challenges in at least a limited range of applications. While there are many gaps in the understanding of much human data and in how observations might be used to benefit patients, the differences in tissue chemistry as detected by in vivo spectroscopy in a

[1] From the GE Research and Development Center, PO Box 8, Schenectady, NY 12301. Received August 29, 1988; accepted October 3. Presented in part as the 1988 David Gould Lecture at The Johns Hopkins University School of Medicine, Baltimore, May 3, 1988. **Address reprint requests to** the author.

very extensive range of disorders ensure its role as a research tool in providing new information about disease processes while offering much hope for extending its role in the diagnostic clinic. Another fine review of spectroscopy (1) and a review of the findings from one major laboratory have recently been published (2).

TECHNICAL FEASIBILITY OF NMR SPECTROSCOPY

Detectability of Chemical Species

To understand what diagnostic value spectroscopy may have in clinical medicine, it is important first to identify what chemistry spectroscopy can detect in the body. The in vivo concentrations, relative NMR sensitivities, and signal-to-noise ratios (S/N) of chemical species that have been or should be detectable in living human tissue (where available) and of several common laboratory substances are compiled in Table 1. Due to the invasive nature of traditional biochemical assays, some of the concentrations are questionable and not all of a species may be detectable by NMR spectroscopy. For example, Siegel et al (12) list brain glutamate values of 6 and 12 mmol/kg in humans and rats, respectively (12–24 mmol/kg in —CH_2— protons), whereas McGilvery (9) cites a value of 3 mmol/kg of glutamate for human brain, and prominent glutamate resonances of amplitude comparable to those of n-AcAsp do not appear in localized water-suppressed human brain spectra (16,26). In fact, the relative amplitudes of rat brain H-1 spectra in studies by Hetherington et al and Rothman et al (13,27) suggest an NMR-visible glutamate concentration of less than 2 mmol/kg if the n-AcAsp and alanine concentrations are correct. So where is all the glutamate in H-1 brain spectra? On the other hand, the phosphorus metabolite levels measured from human brain by means of P-31 NMR spectroscopy (15) are in good agreement with assayed values in rat brain (12).

The relative S/Ns in Table 1 assume a constant detection bandwidth and optimization of the NMR detection coil so that the sample represents the dominant noise source in every case (6,7). The latter assumption results in a linear increase in detected noise with NMR frequency: If the noise source is constant or if coil noise dominates, the relative S/N of nuclei other than hydrogen deteriorates further. Note also that detection bandwidths will vary with nuclear species due to their different chemical shift dispersions. Thus, choices of spectral widths of 200 ppm and 10 ppm typical of C-13 and H-1, respectively, would result in a fivefold larg-

Table 1
Relative NMR Sensitivity in Tissue at Constant Field Strength

NMR Nucleus and Tissue or Substance	Chemical Moiety*	In Vivo Concentration (mol/kg)*	Relative Sensitivity†	Relative S/N†
H-1				
Water	H_2O	111	100	
Muscle	H_2O	88‡	79	
Adipose	Fat-CH_2	96‡	86	
Muscle	Fat-CH_2	~3‡	~3	
	Creatine-NCH_3	~0.1‡	~0.09	
Brain, Heart	Lactate-CH_3	≤75 m§	≤.07	
Brain‖	n-AcAsp-CH_3	15 m	.014	
	Glutamate-CH_2	12 m	.011	
	Glutamine-CH_2	12 m	.011	
	Aspartate-CH_2	2 m	1.8×10^{-3}	
	Taurine-CH_2	1.9 m	1.7×10^{-3}	
	GABA-CH_2	0.8 m	7×10^{-4}	
	Alanine-CH_3	0.8 m	7×10^{-4}	
	Creatine-NCH_3	~20 m	.018	
	Choline-$N(CH_3)_3$	~50 m	0.45	
P-31				
86% phosphoric acid	$\equiv PO_4$	8.8	0.53	1.3
Muscle	PCr	30 m#	1.8×10^{-3}	4.4×10^{-3}
Muscle	β-ATP	5 m#	3×10^{-4}	7.4×10^{-4}
Heart	PCr	~10 m**	5×10^{-4}	1.3×10^{-3}
Brain	PCr	5 m††	3×10^{-4}	7.4×10^{-4}
Brain	β-ATP	3 m††	1.8×10^{-4}	4.4×10^{-4}
Brain	PD	14 m††	8.4×10^{-4}	2.1×10^{-3}
Brain, Muscle	Pi	≤50 m††	$\leq 3 \times 10^{-3}$	$\leq 7 \times 10^{-3}$
C-13				
C-13 ethanol	—(C-13)-H_2—	22	0.32	1.3
Ethanol	—CH_2—	22	3.5×10^{-3}	0.014
Adipose	Fat-CH_2	51‡	8.1×10^{-3}	0.032
Muscle	Fat-CH_2	~1.6‡	2.5×10^{-4}	1×10^{-3}
Liver	Glycogen-C-1	0.3‡‡	4.8×10^{-5}	1.9×10^{-4}
Muscle	Glycogen-C-1	0.09‡‡	1.4×10^{-5}	5.7×10^{-5}
Liver	Glycogen-(C-13)-1	~.03§§	$\sim 4 \times 10^{-4}$	1.7×10^{-3}
Heart	Glutamate-(C-13)-2	≤21 m§§	$\leq 2.9 \times 10^{-4}$	1.2×10^{-3}
	Lactate-(C-13)-3	≤3 m§§	$\leq 4.3 \times 10^{-5}$	1.7×10^{-4}
	Alanine-(C-13)-3	≤6 m§§	$\leq 8.7 \times 10^{-5}$	3.3×10^{-4}
	Aspartate-(C-13)-2	≤12 m§§	$\leq 1.7 \times 10^{-4}$	6.8×10^{-4}
Na-23				
Extracellular	Na^+	0.15‖	5×10^{-3}	.018
Intracellular	Na^+	<.01‖	$<3.3 \times 10^{-4}$	$<1.3 \times 10^{-3}$
F-19				
Liver	PFTB-CF_3[1]	≤1.6##	≤1.2	≤1.3
Brain	Halothane-CF_3	≤5 m***	$\leq 3.4 \times 10^{-3}$	$\leq 4 \times 10^{-3}$
Brain	FDG	~1 m†††	$\sim 8 \times 10^{-4}$	$\sim 8 \times 10^{-4}$
Liver tumor	5-fluorouracil	≤10 m‡‡‡	$\leq 7.5 \times 10^{-3}$	$\leq 8 \times 10^{-3}$

Note.—n-AcAsp = n-acetyl aspartate, GABA = γ-aminobutyrate, PCr = phosphocreatine, Pi = inorganic phosphate, β-ATP = β-adenosine triphosphate, PD = phosphodiesters, PFTB = perfluorotributylamine, FDG = 2-fluoro-2-deoxy-d-glucose, NOE = nuclear Overhauser enhancement.

* Assumes NMR nuclei in moiety are unresolved (isochromatic) and at natural abundance except where isotope specified; isotopically labeled moieties are at 100% isotopic abundance. Natural abundance is 100% for H-1, Na-23, F-19, and 1.108% for C-13 (3). C-13 spectra are H-1 decoupled but without NOE (H-1 NOE ≤3). Na-23 is assumed to be 40% NMR visible (5). mol/kg = moles/per kilogram of all designated NMR nuclei in moiety (eg 2 moles H-1 per mole H_2O). m = milli.

† Sensitivity assumes constant noise (3). S/N assumes sample dominant noise source increasing linearly with frequency (6,7). These are the same for H-1.

‡ Muscle is 79% H_2O, ~2.5% fat. Creatine value based on PCr levels (8,9). Adipose is 80% fat. Fat is 12% hydrogen, 77% carbon (10).

§ Brain hypoxia levels of up to 25 μmol/g (11).

‖ From references 12, 13, 14. Assumes amino acids are 100% NMR visible. Creatine levels based on PCr values (15). NMR-visible choline level based on creatine in reference 16.

\# From reference 8.

** Assumes PCr/ATP ~1.6 (17,18).

†† From reference (15). Maximum Pi assumes complete conversion of muscle ATP, PC_1 (8).

‡‡ Diet dependent. Nominal daytime rest value ~50 g/kg in liver, ~15 g/kg in muscle (9).

§§ Produced by (C-13)-1-glucose perfusion (19,20,21). For liver, assumes 10% of total liver glycogen is labeled.

‖ From references 4, 5.

\#\# Major component of Fluosol 43 artificial blood. Values from rats at 9 d after 30 mL/kg intravenously administered dose 10% vol/vol PFTB (22).

*** Assuming ≤1.7 mmol is in anesthetized rat brain (23).

††† Rough estimate based on a rate of ~0.3 μmol/min/g of tissue FDG utilization (24).

‡‡‡ For doses ≤180 mg/Kg iv in mice (25).

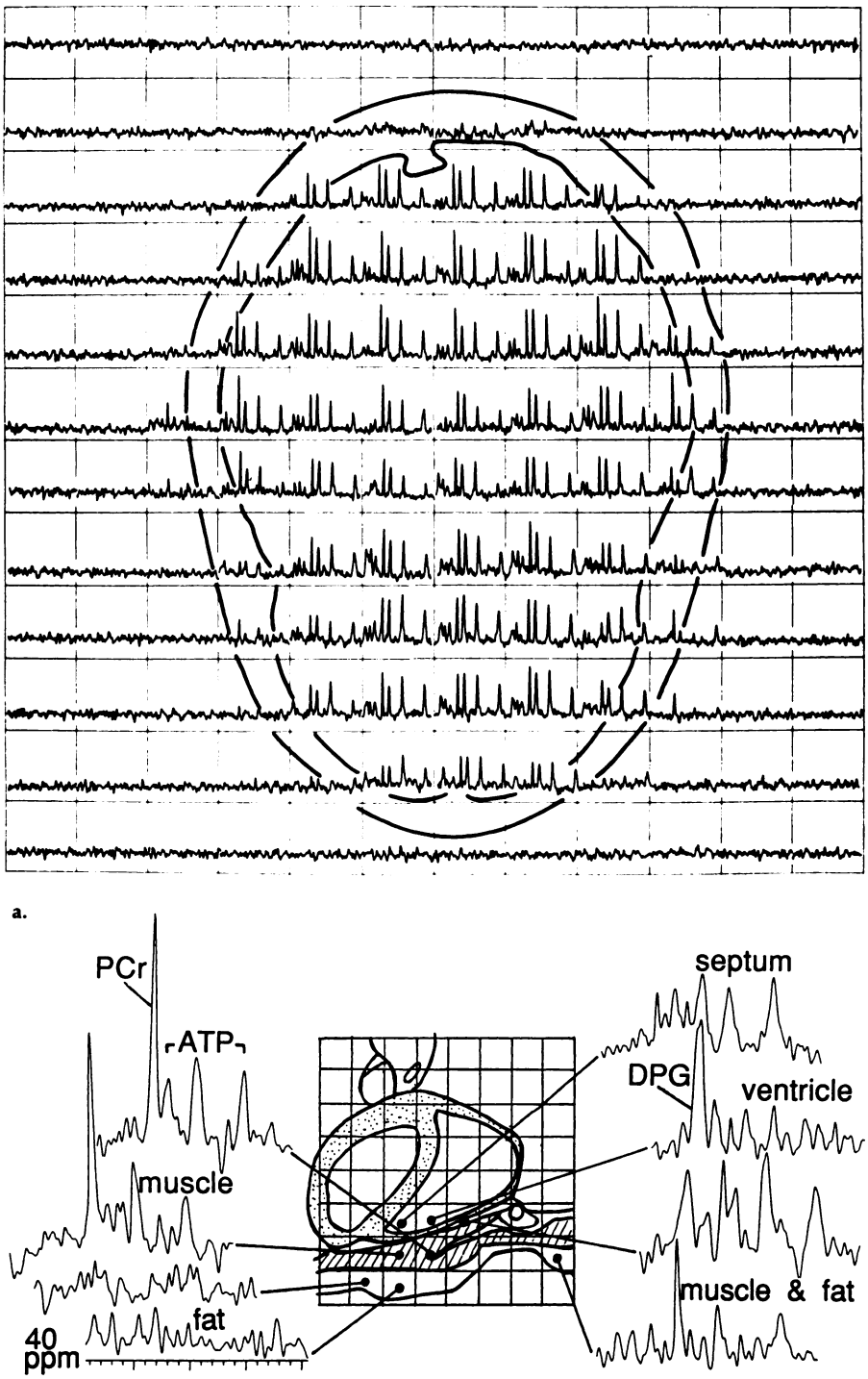

Figure 1. **(a)** P-31 volume spectroscopic image (four-dimensional representation) of the human head acquired from a 5-cm-thick section above the temple with a whole-body 4-T research system (37,38). The spectra are each displayed in their 2 × 2-cm (20 cm^3) voxels outlined by the periphery of the brain and the head as traced from a corresponding H-1 image. Peaks from right to left derive from ATP (β, α, and γ phosphates), PCr, PD, Pi, and PM. **(b)** P-31 spectra from a cardiac-gated spectroscopic image set acquired in 15 minutes with a surface coil on the chest and a conventional 1.5-T system (39). Voxels are again 2 × 2 × 5 cm^3, located relative to the myocardium traced from a H-1 image as indicated. (**a** from P.A. Bottomley and C. J. Hardy, unpublished.)

er detection bandwidth for C-13 at the same field strength (because the C-13 resonant frequency is approximately one-fourth that of H-1), and a corresponding additional $\sqrt{5}$-fold loss in the relative S/N ratio of the C-13 spectrum if no other signal filtering were employed (the final result also depends on the choice of line-broadening filter).

The foregoing caveat notwithstanding, the table reveals several interesting features. First, the present detection limit appears to be remarkably small—around a millionth of that of H-1 in water. How is this possible? At 1.5 T, a 10-cm-diameter H-1 surface coil placed on the body can deliver from water in a single free induction decay (FID) about 80 $Hz^{1/2} \cdot \mu L^{-1}$ of what might be called *intrinsic NMR S/N* (7), because system electronic noise sources are excluded (28). A species of sensitivity 10^{-6} of this is detected by increasing the sample volume, averaging many acquisitions, and reducing the system bandwidth. For example, averaging 10^3 FIDs from 10 mL, rather than a microliter, of sample and reducing the detection bandwidth to one-sixteenth of that employed for H-1 imaging of water results in the requisite million-fold improvement in S/N, thereby permiting access of the insensitive species to state-of-the-art clinical spectroscopic technology (29). Nevertheless, the compromises necessary to compensate for poor sensitivity ensure that such species will never be observed or imaged under the same conditions and with the same quality that H-1 NMR of water in tissue enjoys.

A second feature of the table is that the principal cause of the relatively poor sensitivity and S/N performance of most chemical species is their low concentrations. Compared with water protons at approximately 100 mol/kg, most metabolites exist in millimolar concentrations, thereby accounting for a factor of 10^{-5} of the *sensitivity gap*. And a gap indeed exists in the distribution of concentrations of NMR-visible chemical moieties in tissue. The window of NMR-visible chemistry reveals essentially just water and fat at very high sensitivity, and crucially important tissue metabolites like ATP and lactate at very low sensitivities. Fortuitously absent or aproblematic in H-1 spectra are the many other chemical moieties of intermediate concentrations such as membrane and protein constituents, or phospholipids and bone phosphates in P-31 spectra, which might otherwise confuse and prevent metabolite detection with NMR spectroscopy. The likely reason for this reveals another facet of NMR spectroscopic technique: The in vivo chemical shift experiment is sensitive only to the most mobile of chemical entities in tissue—typically water, energy sources, and some amino acids. Other tissue components existing

in relatively bound states exhibit short spin-spin relaxation times (T2 $\lesssim$ 1 msec) and either do not appear in chemical shift spectra or contribute only a broad baseline hump, which can be removed by signal processing (28,29).

Spatial Localization

Whereas in MR imaging a consensus on the best localization technique evolved rapidly as planar and whole-volume approaches emerged, no such consensus on localization strategy exists for NMR spectroscopy. This is largely because (*a*) the need to average large tissue volumes to gain sufficient sensitivity to detect metabolites argues for minimal localization, and (*b*) the information provided by spectroscopy is chemical rather than anatomic. To recognize these facts is to recognize the necessity of incorporating into the spectroscopic study a conventional anatomic imaging technology for locating the tissues of interest (29). H-1 NMR imaging is an obvious choice for this because both techniques can be performed without moving the patient, and, moreover, because they employ the same physical principles, volumes of interest identified in MR images can be directly and precisely selected for spectroscopy (28).

While there are numerous spectroscopic localization techniques (30), by far the majority of patient spectroscopic data to date derive from just five techniques. These are simple surface coil acquisition (31), rotating frame zeugmatography (RFZ) (32), topical MR (TMR) (33), depth-resolved surface coil spectroscopy (DRESS) (34), image-selected in vivo spectroscopy (ISIS) (35), and one to three dimensional (1-3D) phase encoding gradient or spectroscopic imaging techniques (2-4DFT [Fourier transform]) (36). Nevertheless, this limited range of clinically tested techniques is perhaps more reflective of the availability of local champions to push beyond technique development into applications than it is a real measure of the shortcomings of other techniques.

All localization techniques fall into three general categories: those that achieve localization using spatial gradients in the radio-frequency (RF) excitation or detection fields, as in surface coil and RFZ methods; those that localize by means of static spatial gradients in the main magnetic field, as in the TMR approach; and those that use pulsed spatial gradients at audio frequencies (AF), as exemplified by the DRESS, ISIS, and 2-4DFT methods (28). A detailed account of all the localization techniques is beyond the goals of this paper, but these techniques have been reviewed recently (30). Examples of P-31 3DFT spectroscopic images of the human brain and heart are shown in Figure 1 (37,38,39).

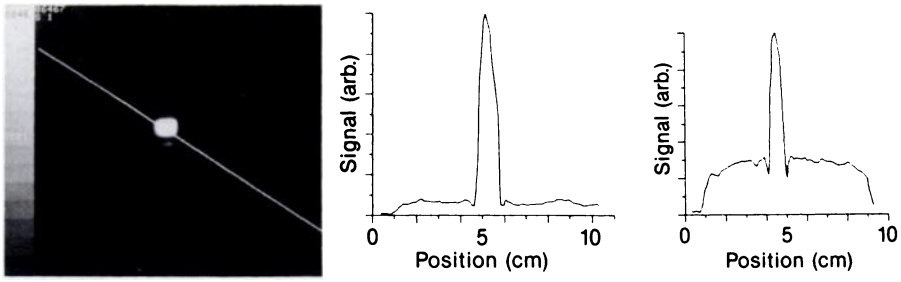

a. b. c.

Figure 2. **(a)** H-1 image of a 6-cm^3 voxel localized in a 450-cm^3 jar of water obtained with a single-voxel three-dimensional localized spectroscopic technique. The image is a direct representation of the spatial sensitivity profile of the localization technique. **(b)** Plot of the signal intensity along the diagonal. Signal from outside the voxel is less than one-tenth the intensity of signal within it. However, in spectroscopic applications, the signal acquired is actually the total integrated response from the sample. **(c)** This is plotted versus the horizontal axis: The total integrated signal from outside the volume is fourfold that of the signal within, so spatial localization of a spectrum is actually very poor. (P. A. Bottomley, C. J. Hardy, and C. L. Dumoulin, unpublished.)

A fundamental, inescapable disadvantage of the RF gradient techniques relative to the pulsed (AF) gradient methods is that the geometry of localized voxels is governed by and varies with the choice of RF coil geometry, which limits choices of RF coils based on anatomic and S/N criteria. Moreover, no RF coil design yet produced can come close to matching simultaneously the spatial gradient performance in all three dimensions achievable by a state-of-the-art x, y, and z MR imaging gradient coil set, expecially without degrading NMR performance. Thus the definition and control of volumes localized by RF gradient techniques are inherently inferior to those of AF gradient techniques. A fundamental disadvantage of static gradient localization techniques is the inferior definition and control of selected voxels. This arises because of the difficulty of generating a magnetic field very uniform across the voxel volume but extremely nonuniform at its periphery, as is necessary to avoid contamination by signals from outside the voxel. Once created, such a field cannot easily be moved from the centre of the coils that produce it, so the subject must usually be moved relative to the magnet if spectra are to be acquired from several locations.

Precise knowledge of the size, location, and content of spectroscopic volumes assumes critical importance for absolute metabolite quantification in moles per kilogram (15), and for studies involving heterogeneous disease and/or mixtures of normal tissue within a selected voxel where it is important to differentiate between changes in anatomy and changes in metabolism. For these reasons and because of the direct proportionality between voxels localized by conventional MR imaging and voxels localized by AF gradients in spectroscopy (gradient strength scales directly with voxel size and gyromagnetic ratio), we have pursued the pulse gradient (AF) techniques (28). Note, however, that a localized spectrum generated by any technique represents an integrated response from the whole sample (28,40). This can include major contributions from outside the selected voxel if these areas constitute a large enough fraction of the sample (40). The size of the sensitive volume from which the spectrum derives is therefore *not* usually well represented by the sensitivity profile or the corresponding NMR image unless these too are integrated. Profiles based on integrated responses assuming uniform samples in uniform main magnetic fields are not yet available for many techniques. Real responses can also vary with sample MR relaxation properties and imperfections in pulses (40). This point is demonstrated in Figure 2.

Finally, there is a valid argument for using minimal or no localization technique for many diseases. The latter include global or relatively unlocalized disorders such as muscular metabolic diseases, ischemic disease in the limbs, dementias, asphyxia, and global trauma in the brain, and

Table 2
Choices of Protocol in Clinical Spectroscopy Research

Protocol Decision	Considerations Affecting Decision
Moiety	(*a*) Biochemistry of suspected disorder, or (*b*) a hypothesis anticipating abnormalities, or (*c*) based on previous empirical findings of abnormalities (*d*) Detectability of moiety
NMR isotope	(*a*) Presence in moiety (*b*) Sensitivity (*c*) Availability of instrumentation
Localization strategy	(*a*) Nature of disease: well localized or unlocalized (*b*) Need for spectra from single or multiple voxels (*c*) Ease of compatibility with an available imaging modality (*d*) Availability of instrumentation (*e*) Susceptibility of the technique to artifacts that would compromise results
Size of voxels	(*a*) Size of pathology, tissue heterogeneity (*b*) Sensitivity
NMR coil	(*a*) Sensitivity: detection coil diameter should be ~distance of coil to deepest tissue of interest (*b*) Constraints due to localization strategy and availability of instrumentation
Scan time	(*a*) Patient tolerance (*b*) Sensitivity per voxel size (*c*) Compatibility with any dynamic studies
Stimulus	(*a*) Pharmacologic, therapeutic, or exercise protocol to stimulate changes in spectra (*b*) Time scale must be compatible with NMR experiment (*c*) Stimulus may introduce excessive spectral artifacts (eg, motion).

large tumors or infarctions that occupy all or most of the sensitive volume of an NMR surface coil. The substantial sensitivity advantage of acquiring spectra from whole volumes compared with much smaller localized volumes could easily outweigh any value in the spatial distribution of spectral information in such disorders, rendering sophisticated localization techniques unnecessary. In other cases, methods that simply eliminate surface tissue contributions (eg, with magnetic computer tape) may be all that is required.

Since all of the MR parameters accessible to MR imaging experiments can also, in principle, be measured on each moiety appearing in the spectroscopic experiment, it is obvious that spectroscopy presents a significantly broader range of options for clinical protocols and decisions than MR imaging. These are summarized in Table 2.

BIOCHEMISTRY AND CLINICAL SPECTROSCOPIC FINDINGS

Fat and Lipid Metabolism

Fat is the greatest reserve of oxidizable fuel in man. It is composed principally of triglycerides that are mobilized in combination with lipoproteins, and hydrolyzed by lipoprotein lipase into the component fatty acids before passing into the interior of adipose cells for storage or muscle cells for direct use.

Due to their high concentrations, fat triglycerides detected as a mobile —CH_2— resonance can be imaged directly at high spatial resolution by H-1 NMR spectroscopy. Such imaging has revealed and permitted quantification of fatty infiltration of the liver in clinical studies of 26 patients (41,42), and has significantly improved, by enhancing contrast, the detection of liver metastases in 40 more patients (43). In bone, H-1 spectroscopic images of H_2O and —CH_2— show elevated water content in marrow in chronic myeloid leukemia (44) and necrosis (45) in vivo. A recent study (46) of four patients with bone marrow leukemia made use of volume-localized spectroscopy in postmortem samples with similar findings. H-1 spectra from patients with Duchenne muscular dystrophy show significant —CH_2— elevations relative to normal (8,47), permitting quantification of the extent of replacement of muscle by fat in the disease (8). While fat —CH_2— can also be imaged directly in man by C-13 NMR spectroscopy (48) and surface coil C-13 spectroscopy confirms its elevation in Duchenne muscular dystrophy (8), the value of C-13 spectroscopy in studies of fat in vivo seems limited to the measurement of the ratio of polyunsaturated to monounsaturated fats in tissue and its diet dependence, using the olefinic carbon (—CH=CH—) C-13 resonances (49,50).

Cancer.—Both H-1 and P-31 NMR spectroscopy have revealed significant disturbances in mobile lipids and phospholipids in tumors. One H-1 study investigated the lipid resonances in water-suppressed spectra of 78 human ovary and colon specimens with and without known metastases, shortly after biopsy (51). Elevations in T2 values of proteolipid —CH_2— resonances in metastatic specimens (T2 > 350 msec) were sufficient to permit their identification as malignant tumors with metastatic potential as opposed to benign tumors, although the benign population was rather poorly represented (four of 51 tumors) with a high incidence of false-positive diagnoses of malignancy. Since (*a*) lipid metabolism is deranged in cancer patients; (*b*) similar elevations in T2 are observed in proteolipid resonances from fractionated plasma of cancer patients (52), indicating that the moiety responsible for elongated T2 relaxation is associated with proteolipid particles shed into the blood pool; and (*c*) the same moiety has been identified as a cancer cell membrane constituent (53,54), there is cause for optimism that this NMR property of the H-1 spectrum is characteristic of metastatic tumors. Ultimately, it might be possible to use spatially localized water-suppressed H-1 spectroscopy of tumors to diagnose their malignancy in vivo, and indeed, preliminary results in human brain are promising (55). These findings are also consistent with the significant, but probably nondiagnostic, reductions in lipid H-1 NMR linewidths of unfractionated plasma from tumor patients reported (56) and discussed recently (57), since the reductions are apparently confounded by hyperlipidemia (58).

Phospholipid metabolism is represented in the in vivo P-31 spectrum principally by resonances broadly ascribed to phosphomonoesters (PM) and phosphodiesters (PD). The PM resonances occur at chemical shifts lying between about 5 and 7.5 ppm relative to PCr and are usually assigned to phosphorylethanolamine (PEt), phosphorylcholine (PCh), and sugar phosphates including blood 2,3-diphosphoglycerate (59,5). The PD resonances occur at around 3 ppm and are attributed to glycerophosphorylcholine (GPC) and glycerophosphorylethanolamine (GPE) (59–61,62,5). The phosphomonoesters PEt and PCh are precursors of phosphatidylethanolamine and phosphatidylcholine, which are major constituents of phospholipids and of myelin in brain, and which are continually degraded into the phosphodiesters GPC and GPE (9). The potential role of

these P-31 NMR-detectable compounds as markers for disturbed membrane metabolism in diseased states was hypothesized in 1984 (63). The total NMR-detectable choline pool is also represented in the H-1 spectrum via its $-N(CH_3)_3$ resonance at around 3.2 ppm (26,16,13,64-70), and at around 54 ppm in C-13 spectra (29).

Elevated PM levels, and to a lesser extent PD levels, are a common, sometimes dramatic (71-74), but by no means universal, feature of in vivo P-31 spectra from human tumors of the liver (75-78), brain (72,75-78), muscle, and many other organs in situ (76,79,80-82). Since PM levels also appear elevated in malignant excised perfused breast cancer cells compared with benign tumor cells (62,83), and in the developing infant brain relative to adult brain (61,59,84), elevations of PM level in tumor spectra likely reflect higher membrane phospholipid metabolism associated with higher tumor cell reproduction and growth rates (62,85). However, Oberhaensli et al found that PM level does not appear to be related to the degree of malignancy of the tissue (72). In neuroblastoma, intracranial lymphoma, non-Hodgkin lymphoma, osteosarcoma, and melanoma, tumor regression in response to radiation therapy has resulted in reductions in PM in their P-31 NMR spectra to near normal levels (1,71,75,80,86,87). However, in some cases because the size of the localized volumes that contribute to the spectra can easily exceed the size of regressing tumors, it is unclear whether the change in PM in response to therapy is a property of the treated tumor cells or results from averaging NMR signal contributions from normal tissue with those of tumor cells whose PM levels are unchanged. Other changes in tumor P-31 spectra are discussed in the section on tumor metabolism (see Table 2).

Other disorders.—Significant elevations in PM level and some increases in PD level have also been reported in postmortem P-31 spectra of brain acid extracts from several Huntington and Alzheimer disease patients (88,89). However, we have as yet been unable to observe with spatially localized P-31 spectroscopy similar perturbations from normal in cortical and underlying brain white matter in nine living patients suffering from Huntington, Alzheimer, or Parkinson diseases, but some elevation in PD level was detected in deeper tissue corresponding principally to white matter in two patients with vascular (Binswanger) dementia (90). Elevations in PD level have also been observed in muscle spectra from six patients with Duchenne muscular dystrophy (47), and in muscle spectra from 15 patients studied with hypothyroid disease (2). In the latter investigation, the PD abnormalities were reversed by means of therapy (2). PD level elevations observed in several hundred P-31 muscle spectra in peripheral vascular disease, however, appear to be just the result of natural aging processes (91). Elevations in PM level of up to fivefold have been reported in the liver in a patient with obstructive jaundice and sclerosing cholangitis (76), a patient with jaundice due to fatty liver and a patient with Caroli syndrome compared with a single healthy subject (92), patients with acute viral or alcoholic hepatitis (73), two hypoglycemic patients suffering glucose-6-phosphatase deficiency (73), and ten patients with cirrhosis (93).

In the heart, spatially localized P-31 spectroscopy of an adult patient with biventricular hypertrophic cardiomyopathy has revealed increased PM and PD levels, while no significant changes were observed in a patient with septal hypertrophy (94). Meanwhile, the observation of dramatically elevated lipid resonances in water-suppressed H-1 spectra from dog hearts with moderately reduced blood flow (95,96) and a published P-31 spectrum showing elevated PM levels in a rejecting transplanted rat heart (97) provide further scope for potential human clinical applications of lipid spectroscopy to the evaluation of jeopardized and viable myocardium.

High-Energy Phosphate Metabolism

On hydrolysis, ATP, adenosine diphosphate (ADP), and PCr produce around 8,000 calories per mole for each pyrophosphate bond, which qualifies them as high-energy phosphates. ATP plays such an important role in transporting energy to so many different biochemical reactions it might be considered the fundamental *energy currency* of the body. Its three P-31 resonances occur at around −2.7 ppm (γ-phosphate), −7.8 ppm (α-phosphate), and −16.3 ppm (β-phosphate) relative to PCr, but the γ- and α- resonances usually also contain contributions from ADP, while nicotinamide adenine dinucleotide (NAD) and reduced NAD (NADH) may also contaminate the α-peak. Thus the β-ATP peak is generally considered the most reliable indicator of tissue ATP levels. The energy released in cleaving one phosphate bond from ATP to form ADP is accompanied by a Pi moiety which resonates between about 3.7 and 5.3 ppm relative to PCr, depending on the intracellular pH. In vivo P-31 spectroscopy is therefore unique in permitting noninvasive tissue pH measurements. These are performed by referring the Pi chemical shifts to a pH titration curve (98). High-energy phosphate is stored as PCr in some (but not all) organs, particularly skeletal muscle (Table 1). It rapidly replenishes short-term ATP deficits without consuming oxygen. Several of these important high-energy metabolic reactions may be summarized (8) as follows:

Short-term (anaerobic) energy sources:

$$ATP \rightarrow ADP + Pi + \text{energy}, \quad (1)$$

$$PCr + ADP \rightarrow ATP + \text{creatine}, \quad (2)$$

$$\text{glycogen} + Pi + ADP \rightarrow ATP + \text{lactic acid}. \quad (3)$$

Long-term (aerobic) energy sources:

$$\text{glucose/glycogen} + ATP + Pi + O_2 \rightarrow ATP + H_2O + CO_2, \quad (4)$$

$$\text{fatty acids} + ADP + Pi + O_2 \rightarrow ATP + H_2O + CO_2. \quad (5)$$

The dramatic depletion of tissue PCr and ATP and corresponding growth in acidic Pi that occur within seconds of ischemia or vigorous exercise (8) is, I believe, the most spectacular demonstration of living biochemistry by noninvasive in vivo spectroscopy.

Creatine, glycogen, lactic acid, and glucose are detectable by H-1 and C-13 NMR spectroscopy; these will be discussed in the next section.

Human clinical studies of the high-energy phosphate metabolism of disease fall into three categories: (*a*) studies of disorders involving abnormalities in processes affecting high-energy phosphate metabolites and their response to various stresses; (*b*) studies of ischemic disease, infarction, and necrosis; and (*c*) studies of tumor metabolism.

Metabolic disorders.—Historically, congenital defects in muscle metabolism represented the first human diseases to be studied by in vivo spectroscopy. This is because they could be performed with the simplest of surface coil technologies and with

smaller magnets capable of accommodating only the limbs (8,99–102). For example, McArdle syndrome is an inborn deficiency in the enzyme phosphorylase, which degrades glycogen into glucose-1-phosphate. This causes excessive PCr use and an absence of lactic acid production with exercise, as well as excessive glycogen levels in tissue. In vivo P-31 NMR spectroscopy thus reveals no fall or an increase in muscular pH, excessive PCr reduction during exercise, and in some cases a significant decrease in resting ATP/(PCr + Pi) ratio compared with normal (99, 103–105). Phosphofructokinase is an enzyme that converts fructose 6-phosphate to fructose 1,6-diphosphate early in the process of converting glycogen and glucose to lactate. Its deficiency causes excess fructose 6-phosphate, manifested as an elevated sugar phosphate resonance in the PM region of the P-31 spectrum, no fall in muscular pH with exercise (8,102,103), reduced resting ATP levels, and slower PCr/Pi recovery from exercise (106). Debrancher (amyloglucosidase) enzyme breaks the last branch (C-6) on glycogen to yield glucose. Its absence causes the accumulation of glycogen with too many branches, and muscle P-31 spectra exhibit increasing, rather than decreasing, pH with exercise (103). NADH-coenzyme Q reductase is linked to ATP and PCr synthesis involving electron transport in mitochondria; its deficiency in patients causes decreased PCr and Pi recovery in P-31 muscle spectra following exercise (2, 101, 107–110). Cytochrome *b* is another mitochondrial electron carrier whose deficiency causes substantial reductions in PCr and PCr/Pi ratios in P-31 muscle spectra (111,112). Regular spectroscopic examinations have been successfully used to monitor the benefit of therapy with vitamins K_3 and C in this disorder (111,112). Phosphoglycerate mutase is an enzyme that shifts the phosphate group on phosphoglycerate to an adjacent carbon, leading eventually to ATP formation in the Embden-Meyerhof pathway. Its deficiency in one patient caused abnormal sugar phosphate (PM) accumulation and a milder drop in pH with exercise compared with normal, as well as a slightly slowed recovery of PCr (110). Other mitochondrial myopathies and neuromuscular diseases have manifested abnormalities in P-31 spectra ranging from reduced PCr, PCr/Pi ratios, or elevated Pi in resting muscle, to prolonged acidosis and ATP recovery from exercise (2,100,103,108,109,113,114). Abnormalities in high-energy phosphates were not apparent in hypophosphatemia (115) and paramyotonia (116).

Today, hundreds of patients suffering muscular disorders have been examined with P-31 NMR spectroscopy (2,109). In Duchenne dystrophy, P-31 spectra from resting muscle show abnormally low overall metabolite concentrations, reduced PCr/ATP and PCr/Pi ratios, abnormally alkaline pH, and an abnormal increase in PD (8,112,117,118). In more than 14 patients suffering prolonged exhaustion and excessive fatigue following a previous viral illness, P-31 NMR spectroscopy has revealed abnormally early and rapid muscular acidosis on exercise (2,119), while denervation and reinnervation following surgey in another 22 cases of neuropathy resulted in changes in Pi levels (2). In 13 patients susceptible to malignant hyperthermia, a disorder triggered by anesthesia, resting muscle PCr/Pi ratios were significantly reduced and recovered more slowly from exercise than normal (120). This suggests that a metabolic defect is involved,and that P-31 spectroscopy might be used for determining patient susceptibility to the disorder (120).

Studies of congenital disorders in other organs include brain P-31 surface coil NMR spectroscopy of congenital cerebral atrophy, propionic acidemia, arginosuccinic acidemia, and meningitis in newborn infants (84,121,122), and a chest surface coil study of two infants with hypertrophic cardiomyopathy (112,123). In the infants with atrophy and meningitis, the PCr/Pi ratios were depressed up to 2·4-fold relative to normal, without any significant accompanying pH reductions (121). The acidemic infants showed grossly abnormal brain spectra with no detectable PCr, ATP, or PD, and a Pi resonance exhibiting a very acidic pH of around 6.4 (122). Infants with abnormally low brain PCr/Pi ratios (normal values are 0.8 ± 0.2 at 28 weeks and 1.1 ± 0.2 at 42 weeks, with 95% confidence limits) had a poor survival prognosis and likelihood of neurologic abnormalities (84). In the cardiomyopathic infants, the PCr/Pi ratios, which were attributed predominately to heart tissue, were as low as half that of two normal control subjects but returned to near normal after intravenous glucose or carbohydrate ingestion in one case (123) and riboflavin in the other (112).

In the liver, two patients deficient in glucose-6-phosphatase (von Gierke disease) exhibited decreases in Pi and elevated sugar phosphate (PM) resonances during hypoglycemia, which returned to normal on glucose ingestion (73). Since the enzyme permits conversion of glucose-6-phosphate to glucose, its deficiency is dangerous because there is no other means of supplying glucose to the brain between meals or for converting lactate to circulating glucose (9). Hemochromatosis, a disorder involving excessive iron deposition in the liver, is manifested as significantly broadened water H-1 and P-31 resonances in five patients studied (73), consistent with the paramagnetic line-broadening effect of iron. In several patients suffering hereditary fructose intolerance, ingestion of small amounts of fructose produced greater increases in sugar phosphates and decreased Pi in liver P-31 spectra than in normal subjects, while reduced Pi recorded in spectra following overnight fasting suggests some slight liver damage associated with the disorder (124). In all of these clinical studies of the liver, spectra were spatially localized using magnetic field (TMR) profiling.

Ischemic disease.—Initial applications of in vivo P-31 spectroscopy to human ischemic disease began with simple surface coil studies of the brain in neonates suffering birth asphyxia, again because of the early availability of small bore superconducting magnets (84,121,122,125–127). Birth-asphyxiated infants characteristically have dramatically reduced PCr/Pi ratios as low as 0.2, depending on severity (121), and commencing 2–9 days after birth (125). No associated changes in pH have been observed (84, 121,122,125,126). Infants with PCr/Pi values below 0.8 have a very bad prognosis for survival and early neurodevelopmental outcome (125,127). However, as their clinical condition improves or with infusions of mannitol, PCr/Pi values increase (121). In these studies since, surface coils provide minimal spatial information, the interesting question of metabolic heterogeneity in the damaged tissue remains (127): Is the phosphate metabolism globally altered in the birth-asphyxiated brain, or is there a mixture of local but more severe metabolic abnormalities interspersed with regions of relatively normal metabolism?

In chronic adult cerebral infarctions in four patients examined with DRESS 10 weeks to 7 years after on-

set, we have seen decreases of up to 40% in the total P-31 NMR metabolite signals compared with *normal* contralateral regions of the patients' brains (61). However, in infarctions there were no significant accompanying changes in metabolite ratios and tissue pH was neutral, in contrast to animal studies, which showed elevated Pi in the acute phase of the injury (128). These results were attributed to a reduction in the total number of metabolically active brain cells, with the remaining viable cells apparently exhibiting normal, ischemia-free, phosphate metabolism (61). The findings have been confirmed in four other patients with chronic stroke (129). In 13 patients with ischemic stroke examined 18 hours to 15 years after the stroke, significant PCr/Pi reductions could also be detected only within the first 7 days; thereafter, metabolite ratios recovered, even though a clinical neurologic deficit persisted in all patients (130). In survivors, acidic pH was detected only within the first 32 hours after the stroke; the pH then became alkaline and subsequently returned to neutral by 10 days (130). One patient suffering cerebral infarction associated with hyperglycemia showed no metabolic recovery up to 6 days after stroke; Pi was the only detectable peak, and pH remained near neutral (131).

From both the infant and adult studies, it seems that the brain does not tolerate abnormal phosphate metabolite ratios for very long following ischemic injury, and that mechanisms exist for neutralizing or eliminating acidic pH produced during acute ischemia or hypoxia in the hours after actual damage has occurred.

Ischemic injury in the heart has posed a series of challenges to the in vivo spectroscopist that typify the problems associated with the clinical introduction of a modality that provides fundamentally new diagnostic information. The challenges we addressed are illustrated in Figure 3. For clinical heart spectroscopy to begin, much fundamental information had to be acquired to *affirmatively* and *explicitly* answer the following questions. First, could P-31 spectroscopy detect metabolic changes and therapeutic response in regionally ischemic isolated animal hearts (132)? Second, with improvements in spatial localization techniques (34,35, 136), could localized P-31 spectra be obtained noninvasively from the normal human heart (127,133,136,

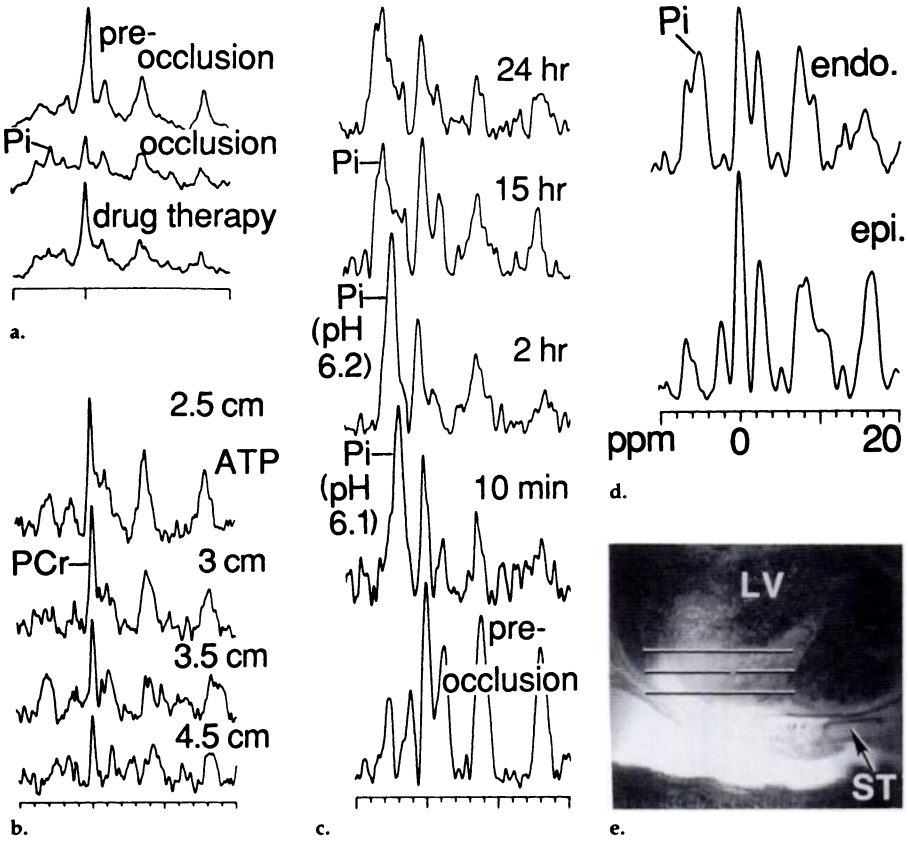

Figure 3. In vivo P-31 spectroscopy in the heart from animal studies to human patients. **(a)** Detection of regional ischemia produced by coronary occlusion (reduced PCr, elevated Pi) and its reversal through drug treatment in isolated perfused rodent hearts (132). Spectra were acquired in about 20 minutes at 4.3 T with a surface coil. **(b)** Noninvasive detection of high-energy phosphate metabolism in normal human heart using DRESS localization (133). Spectra were acquired at 1.5 T in 20 minutes from 1-cm sections as a function of depth from the chest. **(c)** Noninvasive detection and monitoring of regional myocardial ischemia (elevated Pi, reduced pH) after coronary occlusion in dogs using cardiac gated DRESS (134,135). Spectra derive from the same 1-cm-thick section in the anterior left ventricle in about 10 minutes at 1.5 T. **(d)** Altered phosphate metabolism (elevated Pi, top spectrum) in human anterior myocardial infarction 5 days after onset (17). Spectra derive from endocardial (*endo.*) and epicardial (*epi.*) localized sections displaced by 0.5 cm. Acquisition time was 5–7.5 minutes at 1.5 T. **(e)** H-1 surface coil heart image corresponding to **d** with the approximate location of selected volumes indicated (*ST* = sternum, *LV* = left ventricle).

137)? Third, could the localization techniques detect regionally ischemic cardiac metabolism noninvasively in animals (134)? Fourth, bearing in mind the evolution of metabolic changes observed in cerebral infarction and the likelihood of variable delays between the onset of ischemia and the availability of heart patients for P-31 spectroscopic examinations, what is the time course of metabolic changes to be expected in regional myocardial ischemia and infarction (135)? Fifth, after these questions are answered, what is the normal P-31 NMR spectroscopic appearance of human heart (17,94,133,136), and can metabolic changes be detected noninvasively in patients with myocardial infarction (17)? The answer we found to the last question was that the PCr/Pi ratio was significantly reduced and the Pi/ATP ratio elevated in anterior myocardial infarction at 5–9 days after onset in four patients undergoing drug therapy and/or coronary angioplasty (17). The pH, however, was near neutral at these times, consistent with studies in dogs (135). P-31 spectra localized to adjacent myocardium in two patients revealed essentially normal, nonischemic, metabolism (17). Now a final question remains: How can the spectroscopic information from the heart be used to benefit diagnosis or treatment of patients?

In nine (138) and 11 (139) patients suffering congestive heart failure, surface coil P-31 NMR spectroscopy indicates that skeletal muscle metabolism is also compromised. The abnormality is characterized by an elevated resting muscle Pi level (139) and a significantly greater and more rapid PCr level depletion, increase in Pi/PCr ratio, and pH acidification with exercise at all work loads

Table 3
Comparison of Observed Clinical and P-31 Tumor Therapeutic Responses

Host Organ and Tumor Type	Therapy	Clinical Response	P-31 Response	Reference
Bone				
Osteosarcoma	Chemo	Regression	Pi↓, ATP↓, PM↓	80
Osteosarcoma	Chemo	Response, still abnormal	Pi↑, ATP↑, PM↓	80
Osteosarcoma	Chemo	Response, relapse	ATP↑, Pi↑	80
Osteosarcoma	Chemo	Response, relapse	PM↓, Pi↑, ATP↓	80
Osteosarcoma (pelvis)	Rad and chemo	Temporary regression	PCr + Pi↑, PCr/Pi↓	81
Fibrous histiocytoma	Chemo	Improved	ATP↑*, PM↑	149
Ewing tumor	Chemo	Response, still abnormal	Pi↑	80
Non-Hodgkin lymphoma	Chemo	Regression	Normal ATP, Pi, PM	80
Non-Hodgkin lymphoma	Chemo	Regression	PM↑	80
Brain				
Prolactinoma	Chemo	Clinically improved, no change in tumor size	PCr/ATP↓, ATP↓	75
Intracranial lymphoma	Rad	Regression	PM↓, PD↑, PCr↑	75
Astrocytoma, grade 2	Rad	NS	Pi↑, PM↑	75
Oligodendroglioma	Rad	NS	PCr/ATP↑, PCr↑, PM↓	77
Liver				
Neuroblastoma	Rad and Chemo	Regression, tumor reduced	PM/ATP↓	71
Metastasis of uterine adenocarcinoma	Embol	NS	PCr/ATP↓, pH↓, Pi/ATP↑, PD/ATP↓	73
Lymph				
Non-Hodgkin lymphoma (axilla)	Rad	Regression, tumor reduced	PCr/ATP↓, Pi/ATP↓, PD/ATP↓	86
Muscle				
Rhabdomyosarcoma (hand)	Chemo	Worsened	PCr↓, PCr/ATP↓, PCr/Pi↓	79
Rhabdomyosarcoma (thigh)	Rad	Regression, stable	PCr/Pi↓, PCr + Pi↑	81
Neuroectodermal (thigh)	Chemo	Regression	PCr/Pi↓, PD↑, PCr + Pi↑	81
Melanoma (foot)	Chemo	Regression, necrosis	ATP↓, Pi↕, PM↓, PD↓	87
Squamous cell carcinoma (neck)	Rad	Size unchanged	Pi/ATP↑, pH↓, Pi↑, ATP↓	153
Not specified				
Lymphoma (AIDS related)	Chemo	Tumor shrinkage	PM↓	1
25 different cancers	Rad	NS	Changes in PM/ATP, PD/ATP, PCr/ATP, Pi/ATP, pH	82
35 superficial tumors	Rad	Full range	pH fluctuations during therapy (7→7.8)	152

Note.—Rad = radiation, chemo = chemotherapy, embol = embolization, ↑ = value increased, ↓ = value decreased, ↕ = increases and decreases, NS = not specified.
* Exhibited negligible PCr.

(138,139). Similar results have been observed in 11 patients with peripheral vascular disease suffering claudication: Surgical correction in two patients abolished both claudication and spectral differences (140). Many other patients suffering claudication in the legs have been examined with surface coil P-31 spectroscopy (2,141).

Seven excised human kidneys prepared for transplantation (142), a transplanted human kidney in situ (143), and a normal kidney in situ (137) have thus far been studied with localized P-31 spectroscopy. The results from the excised kidneys suggest that high ATP levels and low Pi levels during cold ischemia predict good early graft function (142). Other studies, in animals, of corneas removed for transplantation (144), and transplanted hearts in situ (97,145) where quite dramatic PCr/Pi ratio and PCr/ATP ratio reductions are observed early in cardiac rejection, suggest that P-31 spectroscopy could play an important role in the noninvasive evaluation of human organ viability for transplantation and monitoring their function in situ.

Tumor metabolism.—Tumors are an obvious clinical application for spectroscopy because they usually represent solid masses of abnormal tissue that are clinically manifested only at sizes on the order of 1 cm^3, which are accessible to P-31 NMR spectroscopy (Table 1), and because of the hope that tumor spectra may provide useful diagnostic information (146). The latter hope is based on the facts that the PCr level is, according to the biochemistry, a good indicator of tissue oxygenation state, that the P-31 spectrum provides a measure of the metabolic state of the tumor, and that early in vivo animal studies have shown dramatic spectral changes within hours of radiation therapy (147).

Human in vivo P-31 studies of tumors began with surface coil studies of rhabdomyosarcoma on the hand (79), our own study of malignant glioma in brain (148), studies of liver neuroblastoma in babies (71), and several extremity bone tumors (149), all under a variety of conditions. In the hand, brain, and bone tumors, the high-energy phosphate profile showed significantly lower PCr level, or PCr/ATP ratios compared with those in normal or uninvolved tissue from the same patient. While PCr is not normally found in liver (133), the PM/ATP ratio was highly elevated in neuroblastoma prior to treatment (71). Subsequent in vivo surface coil (81,86,87,149,150) and spatially localized spectroscopy studies (72,74–77,80) of tumor patients have also shown, at first P-31 examination, reduced PCr level or PCr/ATP ratio in non-Hodgkin lymphomas (80,86), B-cell lymphomas (76,80), osteosarcomas (80,81), Ewing sarcomas (80,81,149), melanomas (81,87,150), rhabdomyosarcoma, chondroblastoma, chondrosarcoma, and fibrous histiocytoma (149) tumors in the extremities compared with normal muscle; in squamous cell carcinoma of the tonsil (150), breast (72), and lymph (81) compared with normal muscle; and in brain astrocytomas (72), meningiomas, oligodendrogliomas (72,77), a glioma (77), a prolactinoma, and an intracranial lymphoma (75) compared with normal brain tissue. Like normal liver, hepatoblastoma (72) and carcinoid metastases (74) in liver exhibited no PCr, whereas a liver metastases of a uterine adenocarcinoma did possess PCr, albeit

with a PCr/ATP ratio much lower than that in muscle (72,73). PM/ATP was elevated in all of these liver tumors compared with normal. In six breast cancer patients, total phosphate metabolite contents were three to four times higher than normal (151).

These results provide substantial evidence that PCr level is very often reduced in human tumors compared with their primary host tissue or surrounding tissue at the time that patients typically present and are available for P-31 spectroscopic examination. While a decreased PCr level suggests a more anaerobic tumor metabolism, however, there is little evidence for acute ischemia (high Pi level and low pH). Thus surprisingly, pH is often alkaline, even in tumors with obvious necrosis (72), with values ranging from near neutral to 7.8 (72,73,75–77,79,81,86,152). Pi is elevated only in some brain (72,77) but most extremity bone tumors (80,149). Why is tumor pH elevated? One suggestion, supported by observations of increased pH in mitogenically stimulated cells, is that the pH elevation is related to stimulated growth rates in tumors (72).

Tumor therapy.—Changes in P-31 spectra from human tumors in situ almost invariably occur after chemotherapy, radiation therapy, or embolization therapy. These are very often seen before any variations in tumor anatomy can be detected by other conventional imaging methods and even on time scales as short as 40 minutes after therapy (86). Such observations are extremely encouraging for the potential application of P-31 spectroscopy as an early indicator of therapeutic efficacy. The range of observed responses of tumor P-31 spectra to therapy are summarized in Table 3. As usual, caution is urged in comparing data from different sources, and in particular it should be noted that the timing of the P-31 observations relative to the time of therapy can vary by days. These caveats notwithstanding, the responses, when viewed *en masse*, are highly varied, even among tumors of the same type from the same organ, so that the value of the P-31 spectrum as a predictor of therapeutic response is not currently obvious.

One common response to therapy is decreases in tumor PCr or ATP levels and/or an elevation in Pi level (Table 3). This usually occurs in the absence of tissue acidosis (pH remains elevated) (152) and is usually attributed to an increase in the fraction of hypoxic tumor cells present or to cell death in cases of tumor regression. Unfortunately, however, such hypoxic indicators can also be observed in growing human tumors that are not responsive to therapy (eg, reference 79), while other tumors that do regress show improved or more normal levels of high-energy phosphates after therapy (eg, references 75,149). This is a paradox. Perhaps in some cases spectra from regressing tumors contain proportionately larger contributions from surrounding normal tissue as noted earlier, although similar results have been observed in some animal and cell tumor studies where normal tissue is excluded (154). Important outstanding questions for this application are, Can tumor metabolic response to therapy be distinguished from normal variations in tumor metabolism and from other metabolic responses occurring in surrounding uninvolved tissues due, for example, to the therapy? How specific are metabolic responses to tumor type and therapy type, and how do they vary among individuals? And, most critical for spectroscopy, do tumor metabolic changes provide a measure of therapeutic efficacy? Clearly, there is much exciting work to do.

Glycogen, Glycolysis, the Citric Acid Cycle, and Amino Acids

Many other key metabolic pathways and metabolites are directly accessible to in vivo C-13 and H-1 spectroscopy. For example, glycogen is a polymer used to supply glucose between meals and during heavy muscular exercise. At natural abundance, its six chemically different carbons produce C-13 resonances that are detectable, albeit barely (Table 1), in the normal human liver in situ via surface coil techniques (155) and in muscle. Five of the resonances (at 61, 72, 74, and 78 ppm) are very close or overlap glucose resonances, which are also detectable with C-13 NMR spectroscopy, but the sixth at 100.5 ppm is less ambiguous (156). While no clinical studies of patients have been published at the time this article was completed, metabolic disorders involving abnormalities in tissue glycogen—such as in McArdle syndrome, phosphofructokinase deficiency, and amyloglucosidase deficiency (discussed earlier)—are obvious candidates for C-13 glycogen studies. A C-13 DRESS spectrum from the normal human heart showing glycogen and glucose resonances is depicted in Figure 4.

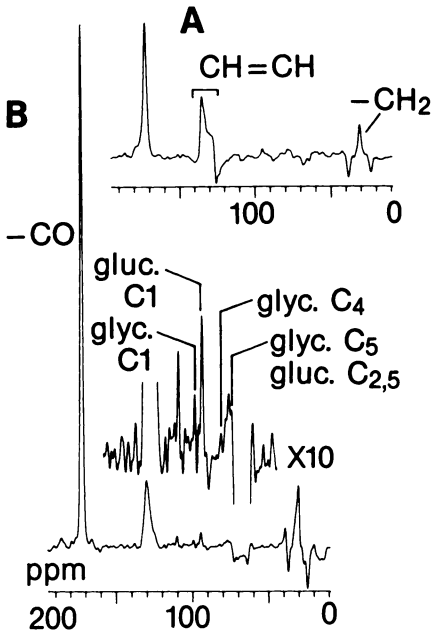

Figure 4. Cardiac gated C-13 DRESS spectra from the human heart acquired without (*A*) and with (*B*) H-1 decoupling and NOE. Spectra derive from a 2-cm-thick section acquired in about 7 minutes at 1.5 T in the anterior myocardium. Insert in *B* magnifies (×10) the region about 100 ppm showing various glucose (*gluc.*) and glycogen (*glyc.*) carbon resonances ($C_{1\text{-}5}$). (P. A. Bottomley, C. J. Hardy, O. M. Mueller, unpublished.)

Energy from 1 mol of glucose in the form of 2 mol of ATP results from its conversion to lactate via glycolysis. Alternatively, 36 mol of ATP can be generated by complete combustion of glucose via the citric acid cycle. These metabolite pathways can be summarized as follows:

Glycolysis:

$$\text{glucose}^*(\rightarrow\text{pyruvate})\rightarrow\text{lactate}^* + \text{ATP}. \quad (6)$$

Citric acid cycle and related reactions:

$$\text{amino acids, carbohydrates, fats} \rightarrow \text{acetylcoenzyme A}, \quad (7)$$

$$\text{glucose}^*(\rightarrow\text{pyruvate}) \rightarrow\text{acetylcoenzyme A}, \quad (8)$$

$$\text{acetylcoenzyme A} \rightarrow \alpha\text{-ketoglutarate}$$
$$\alpha\text{-ketoglutarate} \rightarrow \text{glutamate}^* \leftrightarrow \text{glutamine}^*$$
$$\alpha\text{-ketoglutarate} \rightarrow \text{alanine}^*, \quad (9)$$

$$\text{acetylcoenzyme A} \rightarrow \text{oxaloacetate}$$
$$\text{oxaloacetate} \leftrightarrow \text{aspartate}^*, \quad (10)$$

where asterisks denote species detectable in vivo by H-1 and C-13 spectroscopy. To see lactate, glutamate, aspartate, and alanine with C-13 NMR spectroscopy, a C-13 labeled substrate (eg, C-13 glucose) must be provided intravenously because of

Table 4
Summary of Spectral Abnormalities Detected in Patients in Vivo

Organ and Disorder	Type of Abnormality	References
Muscle		
Enzyme deficiencies, mitochondrial myopathies, Duchenne dystrophy, postviral exhaustion syndrome, malignant hyperthermia susceptibility, hypothyroid disease, claudication, congestive heart failure	At rest: reduced PCr/Pi, PCr/ATP, all P-31 metabolites; elevated Pi, PD, -CH_2- With exercise: slower recovery of metabolites, prolonged acidosis, or elevated or neutral pH, elevated PM	2, 8, 47, 99–114, 117–120, 138–140
Brain		
Infants: asphyxia, atrophy, acidemia, meningitis	PCr/Pi reduced, acidosis (rare)	84, 121, 122, 125, 126, 130
Adults: acute infarction	PCr/Pi reduced in 1st wk, pH reduced in 1st d	130, 131
Chronic infarction	All P-31 metabolites reduced	61, 129, 130
Vascular dementia	Elevated PD	90
Heart		
Infarction	Pi elevated at 5–9 days	17
Cardiomyopathy	PM, PD elevated; PCr/Pi reduced	94, 112, 123
Liver		
Cirrhosis, hepatitis, fatty liver, jaundice	Elevated PM, -CH_2-	41, 42, 73, 76, 92, 93
Enzyme deficiencies	Elevated PM	73
Hemochromatosis	Broad H-1, P-31 lines	73
Fructose intolerance	After fructose ingestion: increased sugar phosphate, reduced Pi	124
Kidney		
Transplants	High ATP/Pi predicts survival	142
Tumors		
Brain, bone, muscle, liver, lymph, breast	Reduced PCr/ATP, creatine, n-AcAsp; elevated Pi, pH, PM, PD, all metabolites, H_2O, lipid T2; after therapy: metabolites return to normal or abnormalities increase or remain unchanged	1, 44, 45, 55, 66, 73–82, 86, 87, 148–153, 159

the low natural isotopic abundance of C-13 (Table 1). The flux and metabolites in the citric acid cycle have been studied by this means in isolated perfused rodent hearts (20,21,157). The results suggest that the C-13 metabolite amplitudes are very sensitive to reduced flow conditions and may vary substantially even before the onset of ischemia can be detected with P-31 NMR spectroscopy (20).

Ischemic disease and cancer.—H-1 NMR spectroscopy can detect lactate, glutamate, and alanine with greater inherent sensitivity than C-13 spectroscopy (Table 1) but with troublesome, often large, contaminating signals from various other —CH_2— and —CH_3 groups. Chemically selective NMR spectroscopic techniques have solved the latter problem, at least in rat brain (13,27) and dog heart (64). Even so, H-1 resonances acquired without such techniques have been assigned to these important metabolites in rat brain spectra (158), and in human in vivo DRESS localized spectra from the brain, liver, and heart (26,159). In one of 3 patients with cerebral infarction, elevated lactate was detected with spatially localized spectroscopy (160), but no lactate elevations were found in four human brain tumors studied in vivo (55). In normal human brain, hyperventilation can also induce lactate increases (70).

In the brain, glutamate and aspartate also serve as the major excitatory inotropic neurotransmitters (12). The major inhibitory neurotransmitter, gamma-aminobutyric acid (GABA), is derived from glutamate via a reaction known as the GABA shunt, which also yields some ATP (12). This and another main inhibitory neurotransmitter, glycine, have been assigned in H-1 spectra from rat and human brain in vivo (27,159,160). N-AcAsp and taurine are other amino acids with suspected neurologic function (12) that are detectable with NMR spectroscopy: The relatively intense —CH_3 resonance of n-AcAsp at 2.0 ppm in H-1 spectra is a good in vivo chemical shift reference when the H_2O signal has been suppressed (26,27,158,160). In four patients with different brain tumors (55), and five patients with large meningiomas (159), and other brain tumors (66), n-AcAsp was either significantly increased or absent in the in vivo tumor spectra compared with its level in uninvolved brain tissue, consistent with the presumption that the tumor performs no neurologic function.

Other amino acids detected with, or at least assigned in, H-1 spectroscopy in normal human tissue in vivo are carnitine, tyrosine, histidine, and tryptophan in liver (67,159); carnitine, carnosine, histidine, and taurine in muscle (68,69); and carnosine, taurine, tyrosine, histidine, tryptophan, and phenylalanine in heart (67,159). Elevations in tryptophan, tyrosine, and phenylalanine have been reported in two patients with liver cancer (67).

The total creatine pool (creatine plus phosphocreatine; see reaction [2]) is also readily detectable in human brain (16,26,55,65,160) and heart (159). Since it is relatively constant, it is useful as a concentration reference in H-1 spectra (158). In meningiomas (159) and other brain tumors (66) it is absent or markedly reduced, consistent with the P-31 results that show reduced PCr in tumors.

Sodium and Fluorinated Pharmaceuticals

Sodium exists in the body in only one chemical form, so Na-23 NMR spectroscopy is usually pointless. However, the sodium does reside in two physically separate compartments: intracellular and extracellular pools. Because the extracellular pool is accessible to agents that can alter the chemical shift of Na-23, spectroscopy can permit the resolution of these two pools into two resonances. Unfortunately, the membrane-impermeable shift reagent, dysprosium, usually used for this purpose in perfused tissue and animal studies (5), can be toxic, and no human in vivo studies have yet been performed. Obvious potential clinical research applications are disorders involving sodium transport or membrane disruption. Na-23 imaging of the human brain without shift reagents and spectroscopic information shows dramatically elevated Na^+ in stroke, hemorrhage, and brain tumors (5,161).

There is very little naturally abundant mobile fluorine in the body, so in vivo F-19 NMR spectroscopy studies are invariably performed on artificially introduced fluorocompounds (162). In vivo animal studies include

fluorinated artificial blood substitutes (22,162), studies of fluorine-bearing anesthetics in brain (23), fluoro-deoxy-glucose metabolism in brain (24) in analogy to positron emission tomography, and the catabolism of fluorine-bearing chemotherapeutic agents in tumors (25). Human in vivo studies monitoring the time of the catabolism of 5-fluorouracil in three patients with tumors have recently been undertaken (163).

CONCLUSIONS

The major thrust of in vivo spectroscopy on patients to date has been in P-31 NMR and high-energy phosphate metabolism, where about a thousand patients have been examined. Table 4 summarizes spectral abnormalities detected in vivo in patients. This establishes the technical feasibility of spectroscopy under clinical conditions. Evidence of abnormalities in P-31 spectra from numerous metabolic disorders, ischemic disease and injury, and tumors throughout the body is substantial, if not overwhelming. In the limited cases where spectral response to therapy was monitored in metabolic and ischemic disorders (2,77,111,112, 121,123,140), successful outcomes were mirrored by improved phosphate metabolism.

More extensive data are available on tumor response to therapy where early changes are very often seen (Table 3). A return of PM levels to normal seems to indicate at least short-term successes in therapy in those tumors that initially exhibit elevated PM. However, changes in high-energy phosphate levels with therapy are highly varied and not well understood, since opposite responses can be associated with the same clinical outcome and vice versa. As abnormalities in P-31 spectra from tumors are shared by other disorders, it does not appear that P-31 spectroscopy can be used for tumor diagnosis alone. The question whether P-31 spectroscopy might be used to distinguish malignant from benign tumors is not yet fully resolved, although one study suggests that spectral abnormalities are unrelated to malignant state (72). Nevertheless, from a biological standpoint, the relative PCr levels provide a measure of tumor oxygenation state, which may be useful in assessing vascularization and planning therapy in some cases.

Metabolic and ischemic disease present the strongest cases for disease diagnosis with in vivo NMR spectroscopy at this stage. In the former, enzymes are not now directly accessible to P-31 spectroscopy because their concentrations are too low. However, the metabolite levels, intracellular pH, and their response to stimuli such as exercise or substrate infusion can be used to characterize or localize the metabolic defect to specific reactions in metabolic pathways. The competing existing diagnostic procedure here is the invasive tissue biopsy, which may not be well tolerated by patients and is ill-suited to dynamic studies requiring many samples. NMR spectroscopy has not yet been evaluated against the tissue biopsy for diagnosing metabolic disease, but it is clear that NMR spectroscopy offers the best and possibly the only hope for performing a *noninvasive* biopsy.

In the case of ischemia, P-31 spectroscopy is unique in its ability to directly measure ischemic metabolic changes in the tissue at risk in vivo. These are characterized by reduced PCr and elevated Pi levels, and acidic pH; tissue possessing these properties may be diagnosed as ischemic. The problem for clinical applications is that ischemia is most often transient: After several hours, ischemic tissue will usually recover by finding alternate nutrient sources, by removal of the original insult or stress, or by therapeutic intervention. Otherwise an infarction will develop wherein cells with inadequate resources die. Thus the time during which spectroscopic diagnoses of ischemia can be made is limited. In life-threatening situations such as acute heart attack or stroke where clinical symptoms are obvious, it remains to be determined specifically how the spectroscopic information could be used to benefit patients directly except as a research probe to compare therapeutic protocols. The most promising clinical applications are therefore in stable patients with suspected ischemia, or in stress test evaluations, for example, in muscle or heart.

In the progression of ischemia to infarction in brain (84,121,122,125-127,130) and heart (17,135), a stage is observed within days of onset where the Pi level remains elevated but pH returns to near neutral. In birth-asphyxiated infants the corresponding reduced brain PCr/Pi ratios are prognostic of survival and neurodevelopmental problems (125,127). Given the kidney and heart transplant data (97,142,145), it is not unreasonable to expect similar prognostic information from other organs. Ultimately the Pi level returns to normal in chronic cerebral infarction with lower overall metabolite levels (61,129). This may provide a quantitative measure of neurologic deficit, although there are other methods of obtaining such information.

Given their relatively high NMR sensitivities in tissue, the H-1 metabolites and amino acids represent a major untapped but potentially highly fertile resource for clinical applications of spectroscopy. The problems have been technical: suppressing water and fat, which dominate H-1 spectra, and distinguishing between metabolites with similar chemical shifts. While water-suppressed H-1 spectra may distinguish brain tumor from normal brain tissue based on the presence of n-AcAsp (55,66,159), tumors can usually be distinguished reliably by conventional imaging. Other tumor lipid studies (51,55) suggest the possibility of assessing malignancy state in vivo by H-1 NMR spectroscopy. Meanwhile, human clinical H-1 studies of metabolites in the citric acid cycle, neurotransmitters, and amino acids in normal and disease states need to be done. C-13, F-19, and Na-23 NMR spectroscopy offer additional noninvasive windows for viewing body chemistry: Investigations are currently still largely in the animal phase, and clinical applications will likely involve the use of spectroscopy *contrast agents* that either generate the NMR signals or enhance the chemical shift dispersion.

In conclusion, the extra dimension of in vivo chemistry that NMR spectroscopy can bring to medicine has both genuine clinical value for diagnosing disease and evaluating therapy, and scientific value as a new source of functional information about the nature of disease states in patients. The field is rapidly evolving: 4-T body magnets improve the quality of spectral information (38), new moieties are being observed, and new parameters such as chemical reaction rates (164) are being measured and imaged in vivo. Indeed, the question of the ultimate clinical utility of spectroscopy will likely reduce to one of extent: Will it serve 0.1% of the patient population that presents for diagnostic imaging evaluations, or 10%—or more? There remains work to do—many pathologic conditions to study and results to understand in terms of biochemistry and the effect on patient treatment. All this points to a very exciting era

of the *coming of age* of clinical NMR spectroscopy. ■

Acknowledgment: I thank C. J. Hardy for fruitful collaboration leading to the results depicted in Figures 1, 2, and 4.

References

1. Weiner MW. The promise of magnetic resonance spectroscopy for medical diagnosis. Invest Radiol 1988; 23:253–261.
2. Radda GK. The use of NMR spectroscopy for the understanding of disease. Science 1986; 233:640–645.
3. Becker ED. High resolution NMR. New York: Academic Press, 1970; 241–251.
4. Lehninger AL. Biochemistry. 2d ed. New York: Worth, 1978; 790.
5. Hilal SK, Maudsley AA, Ra JB, et al. In vivo NMR imaging of sodium-23 in the human head. J Comput Assist Tomogr 1985; 9:1–7.
6. Hoult DI, Lauterbur PC. The sensitivity of the zeugmatographic experiment involving human samples. J Magn Reson 1979; 34:425–433.
7. Edelstein WA, Glover GH, Hardy CJ, Redington RW. The intrinsic signal-to-noise ratio in NMR imaging. Magn Reson Med 1986; 3:604–618.
8. Edwards RHT, Dawson MJ, Wilkie DR, Gordon RE, Shaw D. Clinical use of nuclear magnetic resonance in the investigation of myopathy. Lancet 1982; 1:725–731.
9. McGilvery RW. Biochemistry: a fundamental approach. Philadelphia: Saunders, 1970; 458, 292, 424–429, 307.
10. Snyder WS, Cook MJ, Nasset ES, Karhausen LR, Howells GP, Tipton IH. International Commission on Radiological Protection. Report of the task group on reference man. ICRP no. 23. Oxford: Pergamon, 1984; 110, 42, 289.
11. Behar KL, den Hollander JA, Stromski ME, et al. High-resolution ^{1}H nuclear magnetic resonance study of cerebral hypoxia in vivo. Proc Natl Acad Sci USA 1983; 4945–4948.
12. Siegel GJ, Albers RW, Agranoff BW, Katzman R. Basic neurochemistry. 3d ed. Boston: Little, Brown, 1981; 345, 540, 703, 233–253.
13. Hetherington HP, Avison MJ, Shulman RG. ^{1}H homonuclear editing of rat brain using semiselective pulses. Proc Natl Acad Sci USA 1985; 82:3115–3118.
14. Arus C, Chang Y, Barany M. Proton nuclear magnetic resonance spectra of excised rat brain: assignment of resonances. Physiol Chem Phys Med NMR 1985; 17:23–33.
15. Bottomley PA, Hardy CJ. Precise metabolite assays in vivo? In: Book of abstracts: Society of Magnetic Resonance in Medicine 1988. Vol 2. Berkeley, Calif: Society of Magnetic Resonance in Medicine, 1988.
16. Luyten PR, den Hollander JA. Observation of metabolites in the human brain by MR spectroscopy. Radiology 1986; 161:795–798.
17. Bottomley PA, Herfkens RJ, Smith LS, Bashore TM. Altered phosphate metabolism in myocardial infarction: P-31 MR spectroscopy. Radiology 1987; 165:703–707.
18. Blackledge MJ, Rajagopalan B, Oberhaensli RD, Bolas NM, Styles P, Radda GK. Quantitative studies of human cardiac metabolism by P-31 rotating frame NMR. Proc Natl Acad Sci USA 1986; 4283–4287.
19. Sillerud LO, Shulman RG. Structure and metabolism of mammalian liver glycogen monitored by carbon-13 nuclear magnetic resonance. Biochemistry 1983; 22:1087–1094.
20. Weiss RG, Chacko VP, Glickson JD, Gerstenblith G. Metabolite profile of hibernating myocardium: glucose metabolism is a more sensitive indicator of altered flow than high energy phosphates (forthcoming).
21. Chance EM, Seeholzer SH, Kobayashi K, Williamson JR. Mathematical analysis of isotope labeling in the citric acid cycle with applications to ^{13}C NMR studies in perfused rat hearts. J Biol Chem 1983; 258:13785–13794.
22. Longmaid HE, Adams DF, Neirinckx, RD, et al. In vivo ^{19}F NMR imaging of liver, tumor, and abscess in rats. Invest Radiol 1985; 20:141–145.
23. Evers AS, Berkowitz BA, d'Avignon DA. Correlation between the anesthetic effect of halothane and saturable binding in brain. Nature 1987; 328:157–160.
24. Nakada T, Kwee IL, Conboy CB. Noninvasive in vivo demonstration of 2-fluoro-2-deoxy-d-glucose metabolism beyond the kexokinase reaction in rat brain by ^{19}F nuclear magnetic resonance spectroscopy. J Neurochem 1986; 46:198–201.
25. Stevens AN, Morris PG, Iles RA, Sheldon PW, Griffiths JR. 5-fluorouracil metabolism monitored in vivo by ^{19}F NMR. Br J Cancer 1984; 50:113–117.
26. Bottomley PA, Edelstein WA, Foster TH, Adams WA. In vivo solvent-suppressed localized hydrogen nuclear magnetic resonance spectroscopy: a window to metabolism? Proc Natl Acad Sci USA 1985; 82:2148–2152.
27. Rothman DL, Behar KL, Hetherington HP, Shulman RG. Homonuclear ^{1}H double-resonance difference spectroscopy of the rat brain in vivo. Proc Natl Acad Sci USA 1984; 81:6330–6334.
28. Bottomley PA. A practical guide to getting NMR spectra in vivo. In: Budinger TF, Margulis AR, eds. Medical magnetic resonance imaging and spectroscopy. Berkeley, Calif: Society of Magnetic Resonance in Medicine, 1986; 81–95.
29. Bottomley PA, Hart HR, Edelstein WA, et al. Anatomy and metabolism of the normal human brain studied by magnetic resonance at 1.5 tesla. Radiology 1984; 150:441–446.
30. Aue WP. Localization methods for in vivo NMR spectroscopy. Rev Magn Reson Med 1986; 1:21–72.
31. Ackerman JJH, Grove TH, Wong GG, Gadian DG, Radda GK. Mapping of metabolites in whole animals by P-31 NMR using surface coils. Nature 1980; 283:167–170.
32. Cox SJ, Styles P. Towards biochemical imaging. J Magn Reson 1983; 55:164–169.
33. Gordon RE, Hanley PE, Shaw D, et al. Localization of metabolites in animals using P-31 topical magnetic resonance. Nature 1980; 287;367–368.
34. Bottomley PA, Foster TH, Darrow RD. Depth resolved surface coil spectroscopy (DRESS) for in vivo ^{1}H, ^{31}P, and ^{13}C NMR. J Magn Reson 1984; 59:338–342.
35. Ordidge RJ, Connelly A, Lohman JAB. Image-selected in vivo spectroscopy (ISIS) a new technique for spatially selective NMR spectroscopy. J Magn Reson 1986; 66:283–294.
36. Brown TR, Kincaid BM, Ugurbil K. NMR chemical shift imaging in three dimensions. Proc Natl Acad Sci USA 1982; 79:3523–3526.
37. Bottomley PA, Charles HC, Roemer PB, et al. Human in vivo phosphate metabolite imaging. Magn Reson Med 1988; 7:319–336.
38. Hardy CJ, Bottomley PA, Roemer PB, Redington RW. Rapid ^{31}P spectroscopy on a 4T whole body system. Magn Reson Med 1988; 8:104–109.
39. Bottomley PA, Hardy CJ. ^{31}P spectroscopic imaging of the human heart. (abstr). In: Book of abstracts: Society of Magnetic Resonance in Medicine 1988. Vol 2. Berkeley, Calif: Society of Magnetic Resonance in Medicine, 1988; 834.
40. Bottomley PA, Hardy CJ. PROGRESS in efficient three-dimensional spatially localized in vivo ^{31}P NMR spectroscopy using multidimensional spatially selective (ρ) pulses. J Magn Reson 1987; 74:550–556.
41. Lee JKT, Dixon WT, Ling D, Levitt RG, Murphy WA. Fatty infiltration of the liver: demonstration by proton spectroscopic imaging. Radiology 1984; 153:195–201.
42. Heiken JP, Lee JKT, Sixon WT. Fatty infiltration of the liver: evaluation by proton spectroscopic imaging. Radiology 1985; 157:707–710.
43. Stark DD, Wittenberg J, Middleton MS, Ferrucci JT. Liver metastases: detection by phase-contrast NMR imaging. Radiology 1986; 158:327–332.
44. Sepponen RE, Sipponen JT, Tanttu JI. A method for chemical shift imaging: demonstration of bone marrow involvement with proton chemical shift imaging. J Comput Assist Tomogr 1984; 8:585–587.
45. Matthaei D, Frahm J, Haase A, Schuster R, Bomsdorf H. Chemical-shift-selective magnetic resonance imaging of a vascular necrosis of the femoral head. Lancet 1985; 1:370–371.
46. Irving MG, Brooks WM, Brereton IM, et al. Use of high resolution in vivo volume selected ^{1}H magnetic resonance spectroscopy to investigate leukemia in humans. Cancer Res 1987; 47:3901–3906.
47. Newman RJ, Bore PJ, Chan L, et al. Nuclear magnetic resonance studies of forearm muscle in Duchenne dystrophy. Br Med J 1982; 284:1072–1074.
48. Hasegawa J, Iriguchi N, Ueshima Y, et al. Natural abundance carbon-13 NMR imaging of the human arm. Magn Reson Imaging 1987; 5(suppl 1):46.
49. Canioni P, Alger JR, Shulman RG. Natural abundance carbon-13 nuclear magnetic resonance spectroscopy of liver and adipose tissue of the living rat. Biochemistry 1983; 22:4974–4980.
50. Moonen C, Oberhaensli R, Galloway G, Rajagopalan B, Radda G. Non-invasive measurement of polysaturated fatty acids in human fat by C-13 magnetic resonance spectroscopy. Clin Sci 1985; 68(suppl 2):29p–30p.
51. Mountford CE, Saunders JK, May GL, et al. Classification of human tumors by high-resolution magnetic resonance spectroscopy. Lancet 1986; 1:651–653.
52. Mountford CE, May GL, Wright CL, et al. Proteolipid identified by magnetic resonance spectroscopy in plasma of a patient with borderline ovarian tumor. Lancet 1987; 1:829–834.
53. Wright LC, May GL, Dyne M, Mountford CE. A proteolipid in cancer cells is the origin of their high-resolution NMR spectrum. FEBS Lett 1986; 203:164–168.
54. May GL, Wright LC, Holmes KT, et al. Assignment of methylene proton resonances in NMR spectra of embryonic and transformed cells to plasma membrane triglyceride. J Biol Chem 1986; 315:1369–1376.
55. Luyten PR, Segebarth C, Baleriaux D, den Hollander JA. ^{1}H NMR spectroscopic examination of human brain tumors in situ at 1.5 tesla (abstr). In: Book of abstracts: Society of Magnetic Resonance in Medicine 1987. Vol 2. Berkeley, Calif: Society of Magnetic Resonance in Medicine, 1987; 971.
56. Fossel ET, Carr JM, McDonagh J. Detection of malignant tumors: Water suppressed proton nuclear magnetic resonance spectroscopy of plasma. N Engl J Med 1986; 315:1369–1376.
57. Scott K. Magnetic resonance and cancer: short presentations and discussion concerning the "Fossel test" for cancer. Resonance: Q Newsletter Soc Magn Reson Med 1988; no. 14, pp 2–3.
58. Holmes KT, Mackinnon WB, May GL, et al. Hyperlipidemia as a biochemical basis of magnetic resonance plasma test for cancer. NMR Biomed 1988; 1:44–49.
59. Gyulai L, Bolinger L, Leigh JS, Barlow C, Chance B. Phosphorylethanolamine: the major constituent of the phosphomonoester peak observed by ^{31}P NMR on developing dog brain. FEBS Lett 1984; 178:137–142.
60. Billadello JJ, Gard JK, Ackerman JJH, Gross RW. Determination of intact tissue glycerophosphorylcholine levels by quantitative ^{31}P nuclear magnetic resonance spectroscopy and correlation with spectrophotometric quantification. Anal Biochem 1985; 144:269–274.
61. Bottomley PA, Drayer BP, Smith LS. Chronic adult cerebral infarction studied by phosphorus NMR spectroscopy. Radiology 1986; 160:763–766.
62. Daly PF, Lyon RC, Fanstino PJ, Cohen JS. Phospholipid metabolism in cancer cells monitored by ^{31}P NMR spectroscopy. J Biol Chem. 1987; 262:14875–14878.
63. Burt CT, Ribolow HJ. A hypothesis: noncyclic phosphodiesters may play a role in membrane control. Biochem Med 1984; 31:21–30.
64. Hardy CJ, Dumoulin CL. Lipid and water suppression by selective ^{1}H homonuclear polarization transfer. Magn Reson Med 1987; 5:58–66.
65. Hanstock CC, Rothman DL, Jue T, Shulman RG. Volume-selected proton spectroscopy in the human brain. J Magn Reson 1988; 77:583–588.
66. Bruhn H, Frahm J, Gyngell ML, Merboldt KD, Hanicke W, Sauter R. Localized proton spectroscopy of tumors in vivo: patients with primary and secondary cerebral tumors (abstr). In: Book of abstracts: Society of Magnetic Resonance in Medicine 1988. Vol 1. Berkeley, Calif: Society of Magnetic Resonance in Medicine, 1988; 253.
67. Barany M, Spigos DG, Mok E, Venkatasubramanian PN, Wilbur AC, Langer BG. High resolution proton magnetic resonance spectroscopy of human brain and liver. Magn Reson Imaging 1987; 5:393–398.

68. Keller PJ, Wehrli FW, Schmalbrock P, Hunter WW, Charles C, Flamig D. 1.5 T proton spectroscopy of human muscle in vivo (abstr). In: Book of abstracts: Society of Magnetic Resonance in Medicine 1986. Vol 3. Berkeley, Calif: Society of Magnetic Resonance in Medicine, 1986; 983–984.
69. Barany M, Flamig D, Venkatasubramanian PN, Charles HC. Fat and water suppressed proton spectroscopy (abstr). In: Book of abstracts: Society of Magnetic Resonance in Medicine 1987. Vol 1. Berkeley, Calif: Society of Magnetic Resonance in Medicine, 1987; 384.
70. Luyten PR, van Rijen PC, Berkelbach JW, et al. ^{1}H and ^{31}P NMR measurement of cerebral lactate levels and pH in humans during hyperventilation (abstr). In: Book of abstracts: Society of Magnetic Resonance in Medicine 1987. Works in progress. Berkeley, Calif: Society of Magnetic Resonance in Medicine, 1987; 27.
71. Maris JM, Evans AE, McLaughlin, et al. ^{31}P nuclear magnetic resonance spectroscopic investigation of human neuroblastoma in situ. N Engl J Med 1985; 312:1500–1505.
72. Oberhaensli RD, Hilton-Jones D, Bore PJ, Hands LJ, Rampling BP, Radda GK. Biochemical investigation of human tumors in vivo with phosphorus-31 magnetic resonance spectroscopy. Lancet 1986; 2:8–11.
73. Oberhaensli RD, Rajagopalan B, Galloway GJ, et al. Assessment of human liver disease by P-31 magnetic resonance spectroscopy (abstr). In: Book of abstracts: Society of Magnetic Resonance in Medicine 1986. Vol 2. Berkeley, Calif: Society of Magnetic Resonance in Medicine, 1986; 561–562.
74. Cox IJ, Sargentini J, Calam J, Bryant DJ, Iles RA. Four dimensional phosphorus-31 chemical shift imaging of carcinoid metastases in the liver. NMR Biomed 1988; 1:56–60.
75. Segebarth CM, Baleriaux DF, Arnold DL, Luyten PR, den Hollander JA. MR image-guided P-31 MR spectroscopy in the evaluation of brain tumor treatment. Radiology 1987; 165:215–219.
76. Bailes DR, Bryant DJ, Bydder GM, et al. Localized phosphorus-31 NMR spectroscopy of normal and pathological human organs in vivo using phase-encoding techniques. J Magn Reson 1987; 74:158–170.
77. Heindel W, Bunke J, Steinbrich W. Image-guided localized ^{31}P NMR spectroscopy of the human brain at 1.5 T. Fortschr Rontgenstr 1987; 147:374–378.
78. den Hollander JA, Luyten PR. Image guided localized ^{1}H and ^{31}P NMR spectroscopy of humans. Ann NY Acad Sci 1987; 508:386–398.
79. Griffiths JR, Cady EB, Edwards RHT, McCready VR, Wilkie DR, Wiltshaw E. ^{31}P NMR studies of a human tumor in situ. Lancet 1983; 2:1435–1436.
80. Ross B, Helsper JT, Cox IJ, et al. Osteosarcoma and other neoplasms of bone. Magnetic resonance spectroscopy to monitor therapy. Arch Surg 1987; 122:1464–1469.
81. Semmler W, Gademann G, Bacheret-Baumann P, Zabel HJ, Lorenz WJ, Kaick G. Monitoring human tumor response to therapy by means of P-31 MR spectroscopy. Radiology 1988; 166:533–539.
82. Ng TC, Vijayakumar S, Majors AW, et al. Examination of ^{31}P MRS metabolites and intracellular pH in 25 human neoplasms (abstr). In: Book of abstracts: Society of Magnetic Resonance in Medicine. Vol 1. Berkeley, Calif: Society of Magnetic Resonance in Medicine, 1986; 104.
83. Degani H, Horowitz A, Hzchak Y. Breast tumors: evaluation with P-31 MR spectroscopy. Radiology 1986; 161:53–55.
84. Hamilton PA, Hope PL, Cady EB, Delpy DT, Wyatt JS, Reynolds ROR. Impaired energy metabolism in brains of newborn infants with increased cerebral echodensities. Lancet 1986; 1:1242–1246.
85. Sostman HD, Armitage IM, Fischer JJ. NMR in cancer. I. High resolution spectroscopy of tumors. Magn Reson Imaging 1984; 2:265–278.
86. Ng TC, Vijayakumar S, Majors AW, Thomas FJ, Meaney TF, Baldwin NJ. Response of non-Hodgkin lymphoma to ^{60}Co therapy monitored by ^{31}P MRS in situ. Int J Radiat Oncol 1987; 13:1545–1551.
87. Semmler W, Gademann G, Schlag P, et al. Impact of hyperthermic regional perfusion therapy on cell metabolism of malignant melanoma monitored by ^{31}P MR spectroscopy. Magn Reson Imaging 1988; 6:335–340.
88. Barany M, Chang YC, Ains C, Rustan T, Frey WH. Increased glycerol-3-phosphorylcholine in post-mortem Alzheimer's brain. Lancet 1985; 1:517.
89. Pettegrew JW, Kopp SJ, Minshew NJ, et al. ^{31}P nuclear magnetic resonance studies of phosphoglyceride metabolism in developing and degenerating brain: preliminary observations. J Neuropathol Exp Neurol 1987; 46:419–430.
90. Smith LS, Bottomley PA, Drayer BP, Herfkens RJ. Localized clinical ^{31}P NMR spectroscopy in Huntington's, Parkinsons', Alzheimer's, and Binswanger's diseases (abstr). In: Book of abstracts: Society of Magnetic Resonance in Medicine 1986. Vol 4. Berkeley, Calif: Society of Magnetic Resonance in Medicine, 1986; 1386–1387.
91. Satrustegui J, Berkowitz H, Boden B, et al. An in vivo phosphorus nuclear magnetic resonance study of the variations with age in the phosphodiesters content of human muscle. Mechanisms Aging Dev 1988; 42:105–114.
92. Cox IJ, Bryant DJ, Collins AG, et al. Four-dimensional chemical shift MR imaging of phosphorus metabolites of normal and diseased human liver. J Comput Assist Tomogr 1988; 12:369–376.
93. Ban N, Moriyasu F, Tamada T, et al. In vivo P-31 MR spectroscopic study of cirrhotic liver using a whole body MR imager. Nippon Shokakibyo Gakkai Zasshi 1987; 84:2551–2557.
94. Rajagopalan B, Blackledge MJ, McKenna BJ, Bolas N, Radda GK. Measurement of phosphocreatine to ATP ratio in normal and diseased human heart by ^{31}P magnetic resonance spectroscopy using the rotating frame depth selection technique. Ann NY Acad Sci 1987; 508:321–332.
95. Evanochko WT, Reeves RC, Sakai TT, Canby RC, Pohost GM. Proton NMR spectroscopy in myocardial ischemic insult. Magn Reson Med 1987; 5:23–31.
96. Herfkens RJ, Hedlund LW, Foley D, Brazzamano S, Reimer KA, Coleman RE. Visualization of fat by proton chemical shift imaging in experimental myocardial infarction (abstr). In: Book of abstracts: Society of Magnetic Resonance in Medicine 1985. Vol 1. Berkeley, Calif: Society of Magnetic Resonance in Medicine, 1985; 159–160.
97. Haug CE, Shapiro JI, Chan L, Weil R. P-31 nuclear magnetic resonance spectroscopic evaluation of heterotopic cardiac allograph rejection in the rat. Transplantation 1987; 44:175–178.
98. Gadian DG. Nuclear magnetic resonance and its application to living systems. Oxford: Clarendon, 1982; 27–36.
99. Ross BD, Radda GK, Gadian DG, Rocker G, Esiri M, Falconer-Smith J. Examination of a case of suspected McArdle's syndrome by ^{31}P nuclear magnetic resonance. N Engl J Med 1981; 304:1338–1342.
100. Gadian DG, Radda GK, Ross BD, et al. Examination of a myopathy by phosphorus nuclear magnetic resonance. Lancet 1981; 2:774–775.
101. Radda GK, Bore PJ, Gadian DG, et al. ^{31}P NMR examination of two patients with NADH-CoQ reductase deficiency. Nature 1982; 295:608–609.
102. Chance B, Eleff S, Bank W, Leigh JS, Warnell R. ^{31}P NMR studies of control of mitochondrial function in phosphofructokinase-deficient human skeletal muscle. Proc Natl Acad Sci USA 1982; 79:7714–7718.
103. Ross BD, Radda GK. Application of ^{31}P NMR to inborn errors of muscle metabolism. Biochem Soc Trans 1983; 11:627–630.
104. Argov Z, Bank WJ, Maris J, Chance B. Muscle energy metabolism in McArdle's syndrome by in vivo phosphorus magnetic resonance spectroscopy. Neurology 1987; 37:1720–1724.
105. Lewis SF, Haller RG, Cook JD, Nunnally RL. Muscle fatigue in McArdles' disease studied by ^{31}P-NMR: effect of glucose infusion. J Appl Physiol 1985; 59:1991–1994.
106. Argov Z, Bank WJ, Maris J, Leigh JS, Chance B. Muscle energy metabolism in human phosphofructokinase deficiency as recorded by ^{31}P nuclear magnetic resonance spectroscopy. Ann Neurol 1987; 22:46–51.
107. Hayes DT, Hilton-Jones D, Arnold DL, et al. A mitochondrial encephalomyopathy: a combined ^{31}P magnetic resonance and biochemical investigation. J Neurol Sci 1985; 71:105–118.
108. Arnold DL, Taylor DJ, Radda GK. Investigation of human mitochondrial myopathies by phosphorus magnetic resonance spectroscopy. Ann Neurol 1985; 18:189–196.
109. Radda GK, Taylor DJ, Arnold DL. Investigation of human mitochondrial myopathies by phosphorus magnetic resonance spectroscopy. Biochem Soc Trans 1985; 13:654.
110. Argov Z, Bank WJ, Boden B, Ro YI, Chance B. Phosphorus magnetic resonance spectroscopy of partially blocked muscle glycolysis: an in vivo study of phosphoglycerate mutase deficiency. Arch Neurol 1987; 44:614–617.
111. Eleff S, Kennaway NG, Buist NRM, et al. ^{31}P-NMR study of improvement in oxidative phosphorylation by vitamins K_3 and C in a patient with a defect in electron transport at complex III in skeletal muscle. Proc Natl Acad Sci USA 1984; 81:3529–3533.
112. Chance B, Leigh JS, Smith DS, Nioka S, Clark BJ. Phosphorus magnetic resonance studies of the role of mitochondria in the disease process. Ann NY Acad Sci 1986; 488:140–153.
113. Argov Z, Bank WJ, Maris J, Peterson P, Chance B. Bioenergetic heterogeneity of human mitochondrial myopathies: phosphorus magnetic resonance spectroscopy study. Neurology 1987; 37:257–262.
114. McCully KK, Argov Z, Boden BP, Brown RL, Bank WJ, Chance B. Detection of muscle injury in humans with ^{31}P magnetic resonance spectroscopy. Muscle Nerve 1988; 11:212–216.
115. Smith R, Newman RJ, Radda GK, Stokes M. Young A. Hypophosphataemic osteomalacia and myopathy: studies with nuclear magnetic resonance spectroscopy. Clin Sci 1984; 67:505–509.
116. Lehmann-Horn F, Hopfel D, Rudel R, Ricker K, Kuther G. In vivo P-NMR spectroscopy: muscle energy exchange in paramyotonia patients. Muscle Nerve 1985; 8:606–610.
117. Newman RJ, Bore PJ, Chan L, Gadian D, Styles P, Taylor D, Radda GK. Nuclear magnetic resonance studies of forearm muscle in Duchenne dystrophy. Br Med J 1982; 284:1072–1074.
118. Griffiths RD, Cady EB, Edwards RHT, Wilkie DR. Muscle energy metabolism in Duchenne dystrophy studied by ^{31}P NMR: controlled trials show no effect of allopurinol or ribose. Muscle Nerve 1985; 8:760–767.
119. Arnold DL, Bore PJ, Radda GK, Styles P, Taylor DJ. Excessive intracellular acidosis of skeletal muscle on exercise in a patient with a post-viral exhaustion/fatigue syndrome. Lancet 1984; 1:1367–1369.
120. Olgin J, Argov Z, Rosenberg H, Tuchler M, Chance B. Noninvasive evaluation of malignant hyperthermia susceptibility with phosphorus nuclear magnetic resonance spectroscopy. Anesthesiology 1988; 68:507–513.
121. Cady EB, de L. Costello AM, Dawson MJ, et al. Noninvasive investigation of cerebral metabolism in newborn infants by phosphorus nuclear magnetic resonance spectroscopy. Lancet 1983; 1:1059–1062.
122. Hope PL, Reynolds EOR. Investigation of cerebral energy metabolism in newborn infants by phosphorus nuclear magnetic resonance spectroscopy. Clin Perinatol 1985; 12:261–275.
123. Whitman GJR, Chance B, Bode H, et al. Diagnosis and therapeutic evaluation of a pediatric case of cardiomyopathy using phosphorus-31 nuclear magnetic resonance spectroscopy. J Am Coll Cardiol 1985; 5:745–749.
124. Oberhaensli RD, Rajagopalan B, Taylor DJ, et al. Study of hereditary fructose intolerance by use of ^{31}P magnetic resonance spectroscopy. Lancet 1987; 2:931–934.
125. Hope PL, de L. Costello AM, Cady EB, et al. Cerebral energy metabolism studied with phosphorus NMR spectroscopy in normal and birth-asphyxiated infants. Lancet 1984; 2:366–370.
126. Younkin DP, Delivoria-Papadopoulis M, Leonard JC, et al. Unique aspects of human newborn cerebral metabolism evaluated with phosphorus nuclear magnetic resonance spectroscopy. Ann Neurol 1984; 16:581–586.
127. Chance B, Leigh JS, Nioka S, Sinwell T, Younkin D, Smith DS. An approach to the problem of metabolic heterogeneity in brain. Ann NY Acad Sci 1987; 508:309–320.
128. Bottomley PA, Kogure K, Namon R, Alonso OF. Cerebral energy metabolism in rats studied by phosphorus nuclear magnetic resonance using surface coils. Magn Reson Imaging 1982; 1:81–85.

129. Nunnally RL, Babcock EE, Vaughan JT, Klein DL, Bonte FJ, Walker-Batson D. Examination of brain metabolism in chronic stroke patients: a phosphorus-31 nuclear magnetic resonance study (abstr). In: Book of abstracts: Society of Magnetic Resonance in Medicine 1987. Vol. 2. Berkeley, Calif: Society of Magnetic Resonance in Medicine, 1987; 538.
130. Levine SR, Welch KMA, Helpern JA, Bruce R, Smith MB. Clinical investigation of ischemic stroke by serial 31-phosphorus NMR spectroscopy (abstr). In: Book of abstracts: Society of Magnetic Resonance in Medicine 1987. Vol 2. Berkeley, Calif: Society of Magnetic Resonance in Medicine, 1987; 536.
131. Levine SR, Welch KMA, Helpern JA, et al. Prolonged deterioration of ischemic brain energy metabolism and acidosis associated with hyperglycemia: human cerebral infarction studied by serial ^{31}P NMR spectroscopy. Ann Neurol 1988; 23:416–418.
132. Nunnally RL, Bottomley PA. Assessment of pharmacological treatment of myocardial infarction by phosphorus-31 NMR with surface coils. Science 1981; 211:177–180.
133. Bottomley PA. Noninvasive study of high energy phosphate metabolism in human heart by depth-resolved ^{31}P NMR spectroscopy. Science 1985; 229:769–772.
134. Bottomley PA, Herfkens RJ, Smith LS, et al. Noninvasive detection and monitoring of regional myocardial ischemia in situ using depth resolved ^{31}P NMR spectroscopy. Proc Natl Acad Sci USA 1985; 82:8747–8751.
135. Bottomley PA, Smith LS, Brazzamano S, Hedlund LW, Redington RW, Herfkens RJ. The fate of inorganic phosphate and pH in regional myocardial ischemia and infarction: a noninvasive ^{31}P NMR study. Magn Reson Med 1987; 5:129–142.
136. Blackledge MJ, Rajagopalan B, Oberhaensli RD, Bolas NM, Styles P, Radda GK. Quantitative studies of human cardiac metabolism by P-31 rotating frame NMR. Proc Natl Acad Sci USA 1986; 84:4283–4287.
137. Matson GB, Twieg DB, Karczmar GS, et al. Spatially selected ^{31}P NMR of human organs with surface coils: improvement of ISIS with a composite pulse (abstr). In: Book of abstracts: Society of Magnetic Resonance in Medicine 1987. Berkeley, Calif: Society of Magnetic Resonance in Medicine, 1987; 605.
138. Wilson JR, Fink L, Maris J, et al. Evaluation of energy metabolism in skeletal muscle of patients with heart failure with gated phosphorus-31 nuclear magnetic resonance. Circulation 1985; 71:57–62.
139. Massie BM, Conway M, Yonge R, et al. ^{31}P nuclear magnetic resonance evidence of abnormal skeletal muscle metabolism in patients with congestive heart failure. Am J Cardiol 1987; 60:309–315.
140. Hands LJ, Bore PJ, Galloway G, Morris PJ, Radda GK. Muscle metabolism in patients with peripheral vascular disease investigated by P-31 nuclear magnetic resonance spectroscopy. Clin Sci 1986; 71:283–290.
141. Nishimura T, Imakita S, Naito H, Takamiya M, Matsuo H, Nakayama R. ^{31}P in vivo spectroscopic study by high-field whole body MR system: an application to a case with arteriosclerosis obliterans. Angiology 1987; 38:609–613.
142. Chan L, French ME, Gadian DG, et al. Study of human kidneys prior to transplantation by phosphorus nuclear magnetic resonance. In: Pegg DE, Jacobsen IA, Hals NA, eds. Organ preservation III. Symposium of the Transplantation Society. Lancaster: MTP, 1982; 113–119.
143. Oberhaensli RD, Galloway GJ, Bore PJ, et al. The study of human organs by phosphorus-31 topical magnetic resonance spectroscopy. Br J Radiol 1987; 60:367–373.
144. Lass JH, Medcalf SK, Greiner DO, Glonek T. Preoperative metabolic analysis of donor corneas using magnetic resonance spectroscopy. Cornea 1987; 6:185–189.
145. Canby RC, Evanochko WT, Barrett LV, et al. Monitoring the bioenergetics of cardiac allograph rejection using in vivo P-31 nuclear magnetic resonance spectroscopy. J Am Coll Cardiol 1987; 9:1067–1074.
146. Griffiths JR, Iles RA. NMR studies of tumors. Biosci Rep 1982; 2:719–725.
147. Ng TC, Evanochko WT, Hiramoto RN, et al. ^{31}P NMR spectroscopy of in vivo tumors. J Magn Reson 1982; 49:271–286.
148. Zimmerman RA, Bottomley PA, Edelstein WA, et al. Proton imaging and phosphorus spectroscopy in a malignant glioma. Am J Neuroradiol 1985; 6:109–110.
149. Nidecker AC, Muller S, Aue WP, et al. Extremity bone tumors: evaluation by P-31 NMR spectroscopy. Radiology 1985; 157:167–174.
150. Ng TC, Majors AW, Meaney TF. In vivo MR spectroscopy of human subjects with a 1.4 T whole body MR imager. Radiology 1986; 158:517–520.
151. Ng TC, Grundfest S, Vijayakumar S, et al. Examination of ^{31}P MRS metabolites of normal and cancerous human breast in situ (abstr). In: Book of abstracts: Society of Magnetic Resonance in Medicine 1987. Vol. 1. Berkeley, Calif: Society of Magnetic Resonance in Medicine, 1987; 37.
152. Ng TC, Majors AW, Vijayakumar S, et al. pH of human neoplasms and its alteration in response to radiotherapy measured by ^{31}P MRS in situ. Radiology (in press).
153. Ng TC, Vijayakumar S, Thomas FJ, et al. Evidences of the clinical application of MRS for prognosis of human cancers in response to radiotherapy (abstr). In: Book of abstracts: Society of Magnetic Resonance in Medicine 1986. Vol 1. Berkeley, Calif: Society of Magnetic Resonance in Medicine, 1986; 173–174.
154. Wehrle JP, Li SJ, Rajan SS, Steen RG, Glickson JD. ^{31}P and ^{1}H NMR spectroscopy of tumors in vivo: untreated growth and response to chemotherapy. Ann NY Acad Sci 1987; 508:201–215.
155. Jue T, Lohman JAB, Ordidge RJ, Shulman RG. Natural abundance ^{31}P NMR spectrum of glycogen in humans. Magn Reson Med 1987; 5:377–379.
156. Canioni P, Alger JR, Shulman RG. Natural abundance carbon-13 nuclear magnetic resonance of liver and adipose tissue of the living rat. Biochemistry 1983; 22:4974–4980.
157. Neurohr KJ, Barrett EJ, Shulman RG. In vivo carbon-13 nuclear magnetic resonance studies of heart metabolism. Proc Natl Acad Sci USA 1983; 80:1603–1607.
158. Behar KL, den Hollander JA, Petrof OAC, Hetherington HP, Prichard JW, Shulman RG. Effect of hypoglycemic encephalopathy upon amino acids, high-energy phosphates, and pH in the rat brain in vivo: detection by sequential ^{1}H and ^{31}P NMR spectroscopy. J Neurochem 1985; 44:1045–1055.
159. Barany M, Langer BG, Glick RP, Venkatasubramanian PN, Wilbur AC, Spigos DG. In vivo H-1 spectroscopy in humans at 1.5 T. Radiology 1988; 167:839–844.
160. Luyten PR, Berkelbach VD, Sprenkel PC, van Rijen PC, Tulleken CAF, den Hollander JA. Cerebral lactate detected by localized 1H NMR spectroscopy in patients with cerebral infarction (abstr). In: Book of abstracts: Society of Magnetic Resonance in Medicine 1987. Vol 2. Berkeley, Calif: Society of Magnetic Resonance in Medicine, 1987; 533.
161. Hilal SK, Ra JB, Oh CH, Mun IK, Roschmann P. Clinical sodium imaging: quantitation of extra and intracellular compartments of tumors (abstr). In: Book of abstracts: Society of Magnetic Resonance in Medicine 1987. Vol 1. Berkeley, Calif: Society of Magnetic Resonance in Medicine, 1987; 243.
162. Holland GN, Bottomley PA, Hinshaw WS. ^{19}F magnetic resonance imaging. J Magn Reson 1977; 28:133–136.
163. Wolf W, Silver MS, Albright MJ, Weber H, Reichardt U, Sauer R. A noninvasive study of drug metabolism in patients as studied by ^{19}F NMR of 5-fluorouracil. Ann NY Acad Sci 1987; 508:491–493.
164. Hsieh PS, Balaban RS. ^{31}P imaging of in vivo creatine reaction rates. J Magn Reson 1987; 74:547–579.